Single-molecule RNA detection at depth by hybridization chain reaction and tissue hydrogel embedding and clearing

Sheel Shah[1,2,*], Eric Lubeck[1,*], Maayan Schwarzkopf[3,*], Ting-Fang He[1,*], Alon Greenbaum[3,*], Chang Ho Sohn[1], Antti Lignell[1], Harry M. T. Choi[3], Viviana Gradinaru[3,‡], Niles A. Pierce[3,4,‡] and Long Cai[1,‡]

ABSTRACT

Accurate and robust detection of mRNA molecules in thick tissue samples can reveal gene expression patterns in single cells within their native environment. Preserving spatial relationships while accessing the transcriptome of selected cells is a crucial feature for advancing many biological areas – from developmental biology to neuroscience. However, because of the high autofluorescence background of many tissue samples, it is difficult to detect single-molecule fluorescence in situ hybridization (smFISH) signals robustly in opaque thick samples. Here, we draw on principles from the emerging discipline of dynamic nucleic acid nanotechnology to develop a robust method for multi-color, multi-RNA imaging in deep tissues using single-molecule hybridization chain reaction (smHCR). Using this approach, single transcripts can be imaged using epifluorescence, confocal or selective plane illumination microscopy (SPIM) depending on the imaging depth required. We show that smHCR has high sensitivity in detecting mRNAs in cell culture and whole-mount zebrafish embryos, and that combined with SPIM and PACT (passive CLARITY technique) tissue hydrogel embedding and clearing, smHCR can detect single mRNAs deep within thick (0.5 mm) brain slices. By simultaneously achieving ~20-fold signal amplification and diffraction-limited spatial resolution, smHCR offers a robust and versatile approach for detecting single mRNAs in situ, including in thick tissues where high background undermines the performance of unamplified smFISH.

KEY WORDS: CLARITY, Amplification, Single-molecule RNA

INTRODUCTION

Imaging gene expression levels with single-cell resolution in intact tissues is essential for understanding the genetic programs in many systems, such as developing embryos and dynamic brain circuits. Single-molecule fluorescence in situ hybridization (smFISH) has been the standard tool for detection of individual RNAs in cells

[1]Division of Chemistry and Chemical Engineering, California Institute of Technology, Pasadena, CA 91125, USA. [2]UCLA-Caltech Medical Scientist Training Program, David Geffen School of Medicine, University of California at Los Angeles, Los Angeles, CA 90095, USA. [3]Division of Biology and Biological Engineering, California Institute of Technology, Pasadena, CA 91125, USA. [4]Division of Engineering & Applied Science, California Institute of Technology, Pasadena, CA 91125, USA.
*These authors contributed equally to this work

‡Authors for correspondence (lcai@caltech.edu; niles@caltech.edu; viviana@caltech.edu)

L.C., 0000-0002-7154-5361

(Femino et al., 1998; Raj et al., 2008, 2006; Levsky et al., 2002; Fan et al., 2001). Using smFISH, an mRNA is detected by a probe set containing 20-40 DNA probes, each carrying one or more fluorophores, and each complementary to a different short subsequence (20-50 nt) along the mRNA target. This approach ensures that multiple probes bind the mRNA, generating bright puncta that can be discriminated from background staining resulting from non-specific binding of individual probes. However, background due to sample autofluorescence is significantly higher in tissue samples than in cell culture, making it difficult to robustly detect smFISH signals in tissue. In addition, light scattering caused by deep tissue imaging necessitates probes with higher photon counts than for thin section imaging. Although we have shown that tissue clearing by PACT (passive CLARITY technique) can alleviate autofluorescence and light scattering problems (Chung et al., 2013; Treweek et al., 2015; Yang et al., 2014) while preserving RNA molecules (Yang et al., 2014), a more robust signal amplification strategy is needed to enable multi-color mapping of single mRNAs in deep tissues (Fig. S1).

Attempts have been made to specifically amplify a single mRNA signal, but these tend to suffer from low efficiency and complex protocols (Player et al., 2001). Here, we describe a simple and efficient method for multiplexed single-molecule signal amplification based on the mechanism of hybridization chain reaction (HCR) (Dirks and Pierce, 2004; Choi et al., 2010, 2014). With this approach, short DNA probes complementary to mRNA targets trigger chain reactions in which metastable fluorophore-labeled DNA hairpins self-assemble into tethered fluorescent amplification polymers (Fig. 1A). As with smFISH, each target mRNA is addressed by 20-40 probes complementary to different subsequences along the target to enable discrimination between mRNAs with multiple probes bound and dots resulting from non-specific binding of individual probes. In contrast to previous in situ HCR methods (Choi et al., 2010, 2014), we limit the HCR amplification time to achieve a mean polymer length of ~20-40 hairpins, generating puncta that are bright enough for high sensitivity, yet small enough for diffraction-limited resolution (Fig. S2). Using orthogonal HCR amplifiers programmed to operate independently, straightforward multiplexing is achieved for up to five channels simultaneously (Fig. 1B, Table S1). We term this method single-molecule HCR (smHCR).

RESULTS AND DISCUSSION

To characterize the sensitivity and selectivity of smHCR in cultured cells, we performed a colocalization experiment in which a low-copy target mRNA (Pcdha constant region) was simultaneously detected using three probe sets of 22 probes each (one smFISH set and two smHCR sets), with the probes alternating between the three sets along the target (Table S2). Dots were identified in each channel by applying a threshold following standard methods for
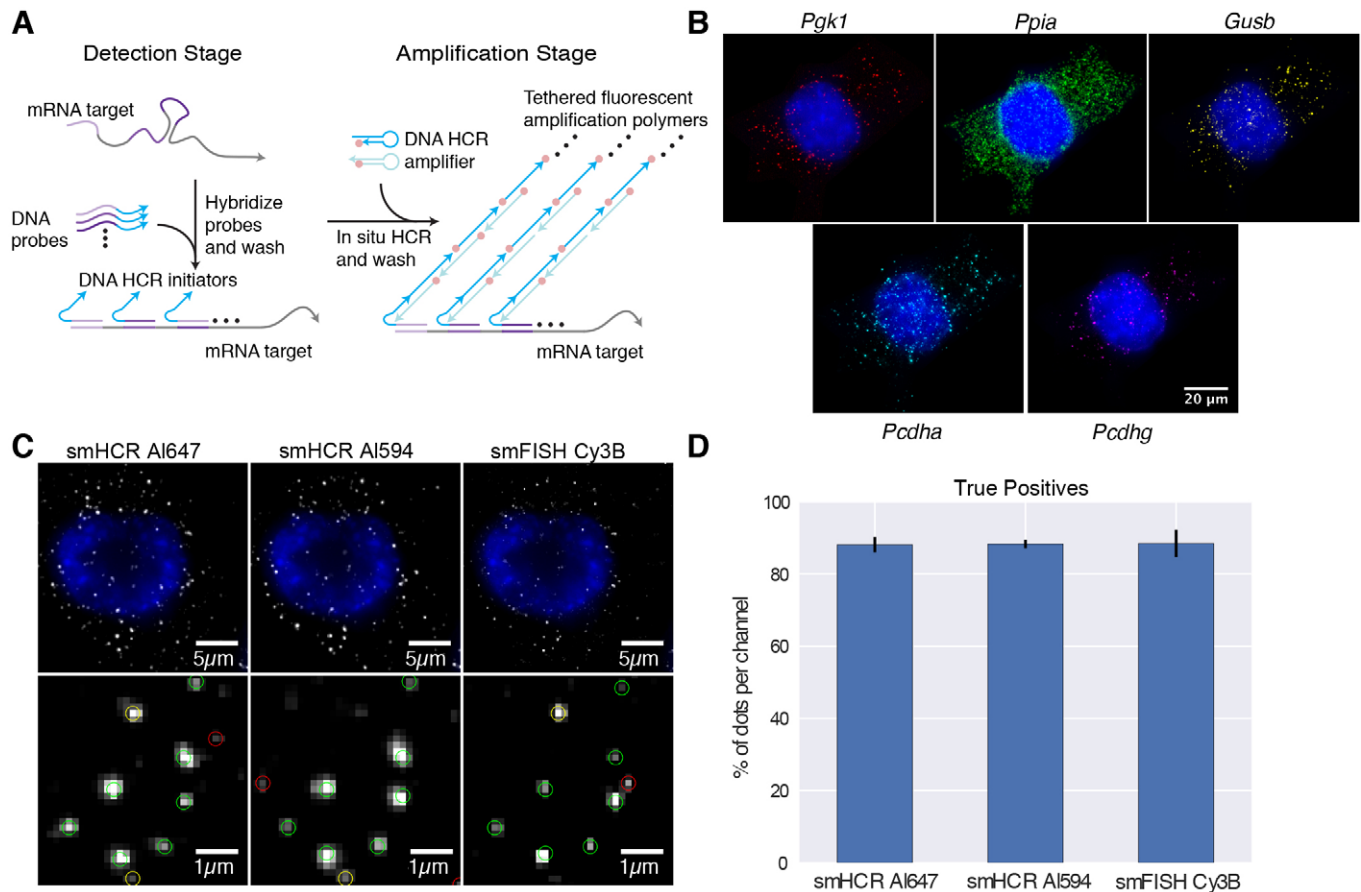
Fig. 1. Single-molecule hybridization chain reaction (smHCR). (A) smHCR protocol. Detection stage: an mRNA target is detected by a probe set containing 20-40 short DNA probes, each binding a 20-30 nt subsequence of the target; each probe in the probe set carries an initiator for the same HCR amplifier. Amplification stage: metastable fluorophore-labeled DNA HCR hairpins penetrate the sample and self-assemble into fluorescent amplification polymers tethered to their initiating probes. The same two-stage protocol is used for multiplexed studies: during the detection stage, all probe sets are introduced simultaneously, each carrying an initiator for an orthogonal HCR amplifier; during the amplification stage, all HCR amplifiers are introduced simultaneously, each labeled with spectrally distinct fluorophores. (B) Simultaneous mapping of five target mRNAs in cultured CAD cells using five spectrally distinct HCR amplifiers (DAPI in blue): *Pgk1* (Cy7), *Ppia* (Alexa Fluor 647), *Gusb* (Alexa Fluor 594), *Pcdha* (Cy3b), *Pcdhg* (Alexa Fluor 488). (C) Comparison of smHCR and smFISH for detection of *Pgk1* via dot colocalization in three channels: smHCR (Alexa Fluor 647), smHCR (Alexa Fluor 594), smFISH (Cy3B). Dots are classified as triple-detected true positives (present in all three channels; green circles), double-detected true positives (present in two out of three channels; yellow circles), or false positives (present in only one channel; red circles). (D) True positive rates for each channel in C (median±median absolute deviation; N=10 wells). Microscopy: epifluorescence. Probe sets for B-D: 22 probes per set, each addressing a 20 nt target subsequence. See Figs S2-S5 for additional data.

smFISH data analysis (Fig. S3A) (Raj et al., 2008). We define true mRNA signals as those dots that are colocalized in at least two of the three channels (Fig. 1C). We calculate a true positive rate for a given channel as the percentage of true mRNA signals detected as dots in that channel. We calculate a false positive rate for a given channel as the percentage of dots in that channel that are not true mRNA signals. For the two smHCR channels and the smFISH channel, the true positive rates are all approximately 88% (Fig. 1D), and the false positive rates are approximately 36%, 27% and 20%, respectively (Fig. S3B). Comparing dot intensities, smHCR provides signal amplification in the region of ~15- to 35-fold relative to smFISH (Fig. S3C,D and Fig. S4), a feature that will become crucial in detecting single transcripts in tissues that have higher levels of autofluorescence.

Notably, in experimental designs where two channels can be allocated to each target mRNA, near-quantitative single-molecule mapping can be achieved (Fig. S5). Using this approach, the threshold for dot identification is lowered in each channel to achieve a higher true positive rate (>95%) at the cost of a higher false positive rate (>60%). Dot colocalization between channels can then

be used to identify the subset of dots that represent true mRNA signals. Alternatively, for the standard situation where each target is detected in only a single channel, and hence colocalization cannot be used for dot classification, the threshold must be raised to reject false positives at the cost of also rejecting some true positives, as is the case for smFISH (Fig. S5) (Raj et al., 2008).

To examine the performance of smHCR within the more challenging imaging setting of an intact vertebrate embryo, we repeated the three-channel colocalization study in a whole-mount zebrafish embryo with confocal imaging. The target mRNA, *kdrl* (a medium-copy target expressed in the endothelial cells of blood vessels), is detected using three smHCR probe sets of 39 probes each, with probes alternating between the three sets along the target mRNA (Table S3). For the three smHCR channels, we observe true positive rates of 86%, 84% and 86% (Fig. 2B), and false positive rates of 36%, 21% and 31% (Fig. S6). To compare the properties of smHCR and smFISH in zebrafish embryos, we disabled HCR amplification in the Alexa Fluor 546 channel by introducing only the first HCR hairpin species, enabling only one hairpin carrying one fluorophore to bind to each probe (smFISH*
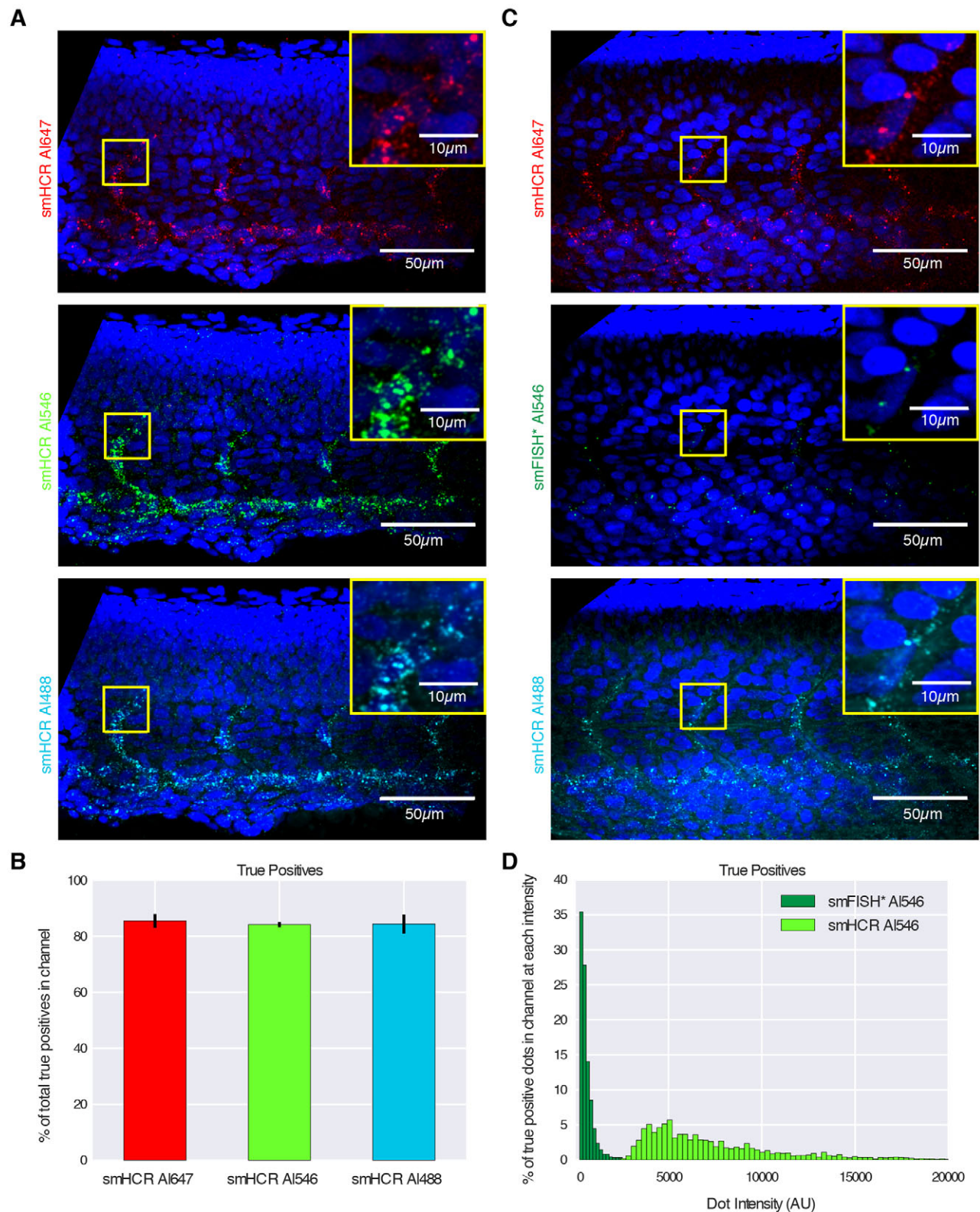
Fig. 2. Imaging single mRNAs within whole-mount zebrafish embryos using smHCR. (A) Dot colocalization in three channels (DAPI in blue): smHCR (Alexa Fluor 647), smHCR (Alexa Fluor 546), smHCR (Alexa Fluor 488). (B) True positive rates for each channel in A (median±median absolute deviation, N=6 embryos). (C) Comparison of smHCR and smFISH* via dot colocalization in three channels: smHCR (Alexa Fluor 647), smFISH* (Alexa Fluor 546), smHCR (Alexa Fluor 488). Channel pairs between A and C are shown with the same contrast; Alexa Fluor 546 images illustrate the difference in intensity between amplified smHCR dots and unamplified smFISH* dots. (D) True positive dot intensities for smHCR (Alexa Fluor 546; N=6 embryos) and smFISH* (Alexa Fluor 546; N=3 embryos). Target mRNA: *kdrl* (expressed in the endothelial cells of blood vessels). Microscopy: spinning disk confocal. Probe sets: 39 probes per set, each addressing a 30 nt target subsequence. Embryos fixed: 27 hpf. See Figs S6-S8 for additional data.

in Fig. 2C; compare the dots in the middle panels of A and C). Comparing the signal intensities of smHCR and smFISH*, we find that the ratio of median dot intensities for smHCR and smFISH* is approximately 15 (Fig. 2D). While the autofluorescence in zebrafish embryos is low enough that unamplified smFISH remains viable (Oka and Sato, 2015; Stapel et al., 2016; Figs S6-S8), automated signal detection is facilitated by the greater signal to background ratio of smHCR.

In the higher background of adult mouse brain sections, smHCR signal amplification becomes essential for robust detection of individual transcripts and is also important when mapping bulk expression in cleared tissue (Sylwestrak et al., 2016). To minimize autofluorescence and light scattering, PACT clearing turns tissues optically transparent and macromolecule-permeable by removing lipids and replacing them with a porous hydrogel, while immersion in RIMS matches the refractive index throughout the sample (Treweek et al., 2015; Yang et al., 2014). We hypothesized that PACT and RIMS combined with smHCR should enable reliable single-molecule imaging at depth within brain samples. As a first test, we used confocal microscopy to image PACT-cleared brain slices at depths up to 84 µm (Fig. 3), performing a three-channel colocalization study using two smHCR probe sets and one smFISH probe set (Table S4). Using smFISH, few dots are visible at a depth of 10 µm, and no signal is evident at a depth of 37 µm (Fig. 3A, bottom). This situation contrasts with the two smHCR channels,

where dots remain bright at a depth of 70 µm (Fig. 3A, middle and top). For each of the two smHCR channels, the true positive rate is approximately >90% (Fig. 3B, top) and the false positive rate is approximately 20% (Fig. 3B, bottom) across the full range of depths. For the smFISH channel, the true positive rate is dramatically lower and the false positive rate is dramatically higher at all depths (Fig. 3B).

To further examine the role of tissue clearing in smRNA detection at depth, we calculated the absolute number of colocalized dots per imaging voxel for pairs of channels with and without PACT (Fig. 3C). Owing to the high level and ubiquitous nature of *Pgk1* expression, two samples when imaged in the same relative locations (layer I-layer II/III of parietal cortex) should show similar transcript numbers per unit volume. With PACT, the two smHCR channels show no measurable decline in colocalized dot count as a function of depth, but without PACT, the dot count decreases at depths beyond ∼15 µm (Fig. 3C left). PACT also significantly reduces the background dot count resulting from autofluorescence (Fig. 3D). Comparisons between smHCR and smFISH emphasize the lack of signal using smFISH (Fig. 3C, right).

Although confocal microscopy rejects out-of-focus background, image acquisition is slow, out-of-plane excitation can photobleach the sample and the imaging depth is limited compared with SPIM. SPIM (Huisken et al., 2004; Dodt et al., 2007; Keller et al., 2010; Tomer et al., 2014; Baumgart and Kubitscheck, 2012) offers a fast
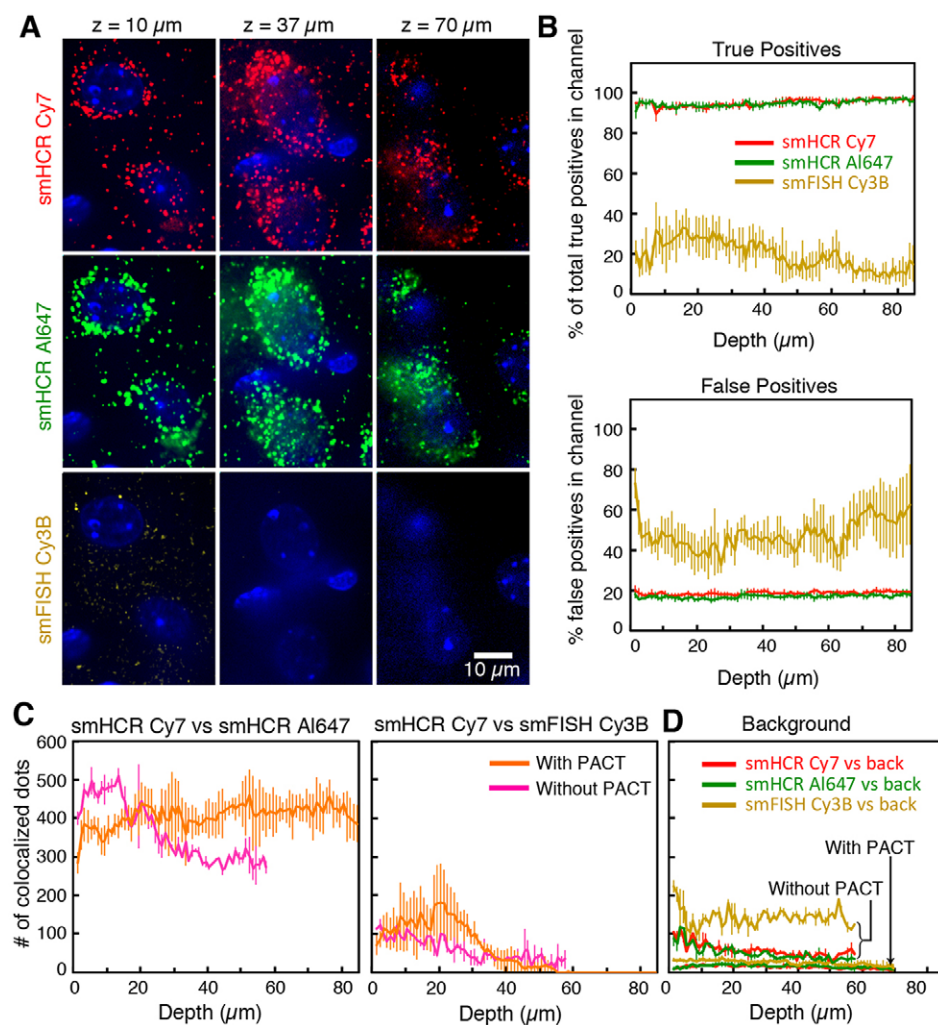

Fig. 3. Imaging single mRNAs in adult mouse brain sections using smHCR and PACT. (A) Dot colocalization in three channels at three depths (DAPI in blue): smHCR (Cy7), smHCR (Alexa Fluor 647), smFISH (Cy3B). Images are displayed with the same contrast within each row. (B) True positive and false positive rates as a function of depth (median ±median absolute deviation, N=8 sections). (C) Effect of PACT clearing on the absolute number of colocalized dots for pairs of channels as a function of depth within a 110×110×1 µm voxel (median±median absolute deviation, N=8 sections with PACT, N=3 sections without PACT). (D) Characterization of background with and without PACT via colocalization of dots in any of three channels with dots due solely to autofluorescence in a fourth channel (excitation at 589 nm) (median±median absolute deviation, N=6 sections with PACT, N=3 sections without PACT). Target: *Pgk1*. Microscopy: spinning disk confocal. Probe sets: 22 or 23 probes per set, each addressing a 20 nt target subsequence. See Fig. S9 for additional data.
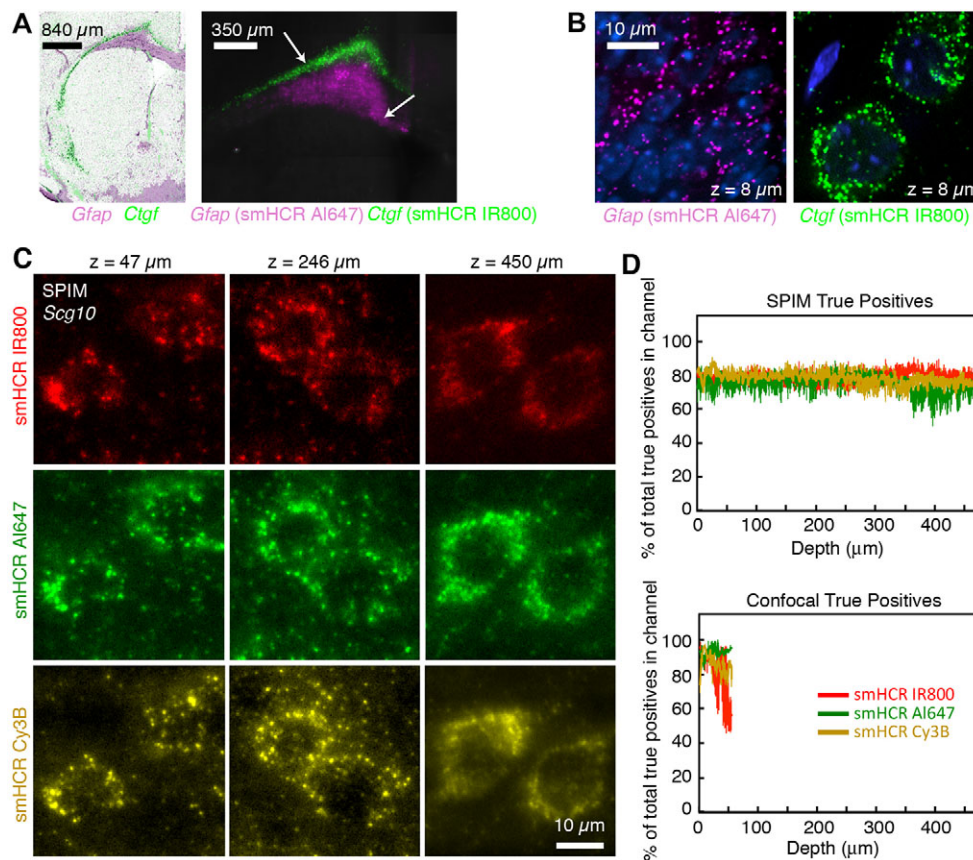
Fig. 4. Imaging single mRNAs in thick adult mouse brain sections using smHCR, PACT and SPIM. (A) *Ctgf* and *Gfap* expression based on: reference Allen Brain Atlas (ABA) composite (*Ctgf*-RP_040407_02_H07-coronal slice #16 and *Gfap*-RP_Baylor_253913 coronal slice #16, sections were selected and overlaid based on the ventricle outline) (left panel) and two-channel smHCR with PACT and SPIM (right panel). Images were generated by stitching together tiled fields of view (1.2×1.2 mm) acquired in SPIM. The SPIM image shows a maximum intensity projection of a 250 μm stack of images. Consistent with the ABA-based overlay, the SPIM images show *Ctgf* highly expressed in the deepest cortical layer and *Gfap* expressed in the white matter astrocytes. (B) High-magnification confocal images at two locations within the same sample (approximate locations denoted by arrows in A). DAPI in blue. (C) *Scg10* mRNA imaged in three channels at three depths using smHCR (IR800, Alexa Fluor 647, Cy3B), PACT and SPIM. (D) True positive rates as a function of depth (median± median absolute deviation, N=3 sections from different brains) using SPIM or confocal imaging of *Scg10*. Probe sets: 20 probes per set, each addressing a 20 nt target subsequence. See Fig. S10 and Movie 2 for additional data.

alternative (∼100 times faster than confocal microscopy) that rejects out-of-focus noise by illuminating and capturing images only from a thin selective plane, typically on the order of 1-10 μm. As smFISH signal is undetectable with SPIM, if SPIM, PACT and smHCR are compatible, it would become feasible to efficiently perform phenotypical studies with single-molecule resolution while preserving the natural long-range architecture of thick samples. To examine the performance of SPIM, PACT and smHCR, we first mapped the expression patterns for two mRNAs (*Ctgf* and *Gfap*) in 250 μm brain slices, recapitulating the large-scale reference patterns in the Allen Brain Atlas (ABA) (Fig. 4A and Movie 1), but now with single-molecule resolution (Fig. 4B). To further characterize SPIM performance, we mapped single *Scg10* mRNAs (a medium to high copy number target) at depths up to 0.5 mm in PACT-cleared brain slices (Fig. 4C and Movie 2). Examining true positive (Fig. 4D) and false positive (Fig. S10) rates for three smHCR channels reveals that SPIM extends the sensitivity and selectivity achieved with confocal microscopy to significantly greater depths (see Figs S11 and S12 for an illustration of image analysis and dot classification for smHCR/PACT/SPIM data in thick samples). Additional studies mapping a high-copy transgenic mRNA in 1 mm brain slices from Thy1-EYFP mice revealed strong and selective HCR signal at depth (Figs S13-S16 and Movie 3), although in this case the expression level of the target was too high to resolve individual dots. Notably though, as PACT-cleared tissue retains endogenous YFP fluorescence, we were able to directly test the selectivity of HCR signal without the need for parallel antibody staining; we observe a one-to-one correspondence between cells labeled by YFP protein fluorescence and cells expressing YFP mRNA by smHCR.

In conclusion, we have shown that smHCR provides a robust method to map single mRNAs of varying abundance in diverse samples. In combination with PACT and SPIM, smHCR enables efficient mapping of single transcripts in thick brain slices, allowing the spatial architecture of the tissue to be preserved. Noting that whole bodies and a wide range of tissues, including human, have been successfully cleared (Treweek et al., 2015; Yang et al., 2014), we expect the combination of smHCR, PACT and SPIM to enable molecular profiling of a wide variety of samples with single-cell and, if desired, single-transcript resolution while preserving geometry and connectivity information. As smHCR is compatible with sequential hybridization methods that we have previously developed (Lubeck et al., 2014; Lubeck and Cai, 2012), it should be possible to perform highly multiplexed studies within thick autofluorescent samples, mapping single mRNAs at depth.

MATERIALS AND METHODS
Sample preparation
Whole-mount zebrafish embryos were prepared using a protocol adapted from Choi et al. (2014). Mouse CNS-derived CAD cells and adult mouse brain sections up to 1 mm thick were prepared using standard techniques as described in supplementary Materials and Methods.

In situ hybridization
smFISH and smHCR probe preparation, and specific hybridization conditions for cultured cells, zebrafish and mouse brain sections are described in supplementary Materials and Methods.

Passive CLARITY technique
Paraformaldehyde-fixed mouse brain slices were PACT cleared before imaging following a previously reported protocol (Yang et al., 2014; Treweek et al., 2015) as detailed in supplementary Materials and Methods.

DEVELOPMENT

Imaging

Epifluorescence microscopy, spinning disk confocal microscopy or SPIM was carried out on cultured cells, whole-mount zebrafish and adult mouse sections as described in supplementary Materials and Methods.

Image processing and analysis

All image analysis of cultured cells, whole-mount zebrafish and adult mouse sections was performed on three-dimensional image stacks in MATLAB as detailed in supplementary Materials and Methods.

Data availability

Movies are available from Dryad at http://datadryad.org/resource/doi:10.5061/dryad.31r0d.

Supplementary information

Supplementary information available online at
http://dev.biologists.org/lookup/doi/10.1242/dev.138560.supplemental

References

Baumgart, E. and Kubitscheck, U. (2012). Scanned light sheet microscopy with confocal slit detection. *Optics Express* **20**, 21805-21814.

Choi, H. M. T., Chang, J. Y., Trinh, L. A., Padilla, J. E., Fraser, S. E. and Pierce, N. A. (2010). Programmable in situ amplification for multiplexed imaging of mRNA expression. *Nat. Biotechnol.* **28**, 1208-1212.

Choi, H. M. T., Beck, V. A. and Pierce, N. A. (2014). Next-generation in situ hybridization chain reaction: higher gain, lower cost, greater durability. *ACS Nano* **8**, 4284-4294.

Chung, K., Wallace, J., Kim, S.-Y., Kalyanasundaram, S., Andalman, A. S., Davidson, T. J., Mirzabekov, J. J., Zalocusky, K. A., Mattis, J., Denisin, A. K. et al. (2013). Structural and molecular interrogation of intact biological systems. *Nature* **497**, 332-337.

Dirks, R. M. and Pierce, N. A. (2004). Triggered amplification by hybridization chain reaction. *Proc. Natl. Acad. Sci. USA* **101**, 15275-15278.

Dodt, H.-U., Leischner, U., Schierloh, A., Jährling, N., Mauch, C. P., Deininger, K., Deussing, J. M., Eder, M., Zieglgänsberger, W. and Becker, K. (2007). Ultramicroscopy: three-dimensional visualization of neuronal networks in the whole mouse brain. *Nat. Methods* **4**, 331-336.

Fan, Y., Braut, S. A., Lin, Q., Singer, R. H. and Skoultchi, A. I. (2001). Determination of transgenic loci by expression FISH. *Genomics* **71**, 66-69.

Femino, A. M., Fay, F. S., Fogarty, K. and Singer, R. H. (1998). Visualization of single RNA transcripts in situ. *Science* **280**, 585-590.

Huisken, J., Swoger, J., Del Bene, F., Wittbrodt, J. and Stelzer, E. H. K. (2004). Optical sectioning deep inside live embryos by selective plane illumination microscopy. *Science* **305**, 1007-1009.

Keller, P. J., Schmidt, A. D., Santella, A., Khairy, K., Bao, Z., Wittbrodt, J. and Stelzer, E. H. K. (2010). Fast, high-contrast imaging of animal development with scanned light sheet-based structured-illumination microscopy. *Nat. Methods* **7**, 637-642.

Levsky, J. M., Shenoy, S. M., Pezo, R. C. and Singer, R. H. (2002). Single-cell gene expression profiling. *Science* **297**, 836-840.

Lubeck, E. and Cai, L. (2012). Single cell systems biology by super-resolution imaging and combinatorial labeling. *Nat. Methods* **9**, 743-748.

Lubeck, E., Coskun, A. F., Zhiyentayev, T., Ahmad, M. and Cai, L. (2014). Single-cell in situ RNA profiling by sequential hybridization. *Nat. Methods* **11**, 360-361.

Oka, Y. and Sato, T. N. (2015). Whole-mount single molecule FISH method for zebrafish embryo. *Sci. Rep.* **5**, 8571.

Player, A. N., Shen, L.-P., Kenny, D., Antao, V. P. and Kolberg, J. A. (2001). Single-copy gene detection using branched DNA (bDNA) in situ hybridization. *J. Histochem. Cytochem.* **49**, 603-612.

Raj, A., Peskin, C. S., Tranchina, D., Vargas, D. Y. and Tyagi, S. (2006). Stochastic mRNA synthesis in mammalian cells. *PLoS Biol.* **4**, e309.

Raj, A., van den Bogaard, P., Rifkin, S. A., van Oudenaarden, A. and Tyagi, S. (2008). Imaging individual mRNA molecules using multiple singly labeled probes. *Nat. Methods* **5**, 877-879.

Stapel, L. C., Lombardot, B., Broaddus, C., Kainmueller, D., Jug, F., Myers, E. W. and Vastenhouw, N. L. (2016). Automated detection and quantification of single RNAs at cellular resolution in zebrafish embryos. *Development* **143**, 540-546.

Sylwestrak, E. L., Rajasethupathy, P., Wright, M. A., Jaffe, A. and Deisseroth, K. (2016). Multiplexed intact-tissue transcriptional analysis at cellular resolution. *Cell* **164**, 792-804.

Tomer, R., Ye, L., Hsueh, B. and Deisseroth, K. (2014). Advanced CLARITY for rapid and high-resolution imaging of intact tissues. *Nat. Prot.* **9**, 1682-1697.

Treweek, J. B., Chan, K. Y., Flytzanis, N. C., Yang, B., Deverman, B. E., Greenbaum, A., Lignell, A., Xiao, C., Cai, L., Ladinsky, M. S. et al. (2015). Whole-body tissue stabilization and selective extractions via tissue-hydrogel hybrids for high resolution intact circuit mapping and phenotyping. *Nat. Prot.* **10**, 1860-1896.

Yang, B., Treweek, J. B., Kulkarni, R. P., Deverman, B. E., Chen, C.-K., Lubeck, E., Shah, S., Cai, L. and Gradinaru, V. (2014). Single-cell phenotyping within transparent intact tissue through whole-body clearing. *Cell* **158**, 1-14.

DEVELOPMENT

Supplementary Materials and Methods

Cultured cells

Sample Preparation

CAD cells were obtained from Sigma Aldrich (Sigma, Cat. # 08100805) cultured as described previously (Suri et al., 1993). CAD cells were grown in DMEM/F-12 medium (ThermoFisher, Cat. # 12634), supplemented with 10% FBS (Gibco, Cat. # 16000) and 1% penicillin-streptomycin (Gibco, Cat. # 15140) on standard tissue culture flasks in a humidified 5% CO_2 incubator. CAD cells were passaged every 3 to 4 days and cells were plated at a 1:10 dilution. For microscopy experiments, 22 mm × 40 mm no. 1.5 coverslips (EMS, Cat. # 72204) were coated with 0.01% poly-D-lysine (Sigma, Cat. # P7280) for 2 hours at 37 °C in standard tissue culture dishes. Coverslips were washed with UltraPure water (ThermoFisher, Cat. # 10977) and cells were plated on the coverslip at a 1:6 dilution. Cells were grown overnight and fixed the following day with 4% formaldehyde in 1× PBS for 15 minutes at room temperature. Formaldehyde was then washed out with RNAse-free 2× SSC and stored in 70% ethanol and stored at -20ºC.

In situ hybridization

Probe design and synthesis

DNA 20-nt probes complementary to the target mRNA were designed using Stellaris Designer (Tables S1 and S2). For smFISH probes, 5' amine modified oligos were purchased and were directly coupled to a fluorophore and purified as described in Lubeck and Cai, 2012. smHCR probes are 60-nt long with a 20-nt long mRNA recognition sequence, 4-nt spacer and a 36-nt HCR initiator on the 3` end.

Probe hybridization

Coverslips coated with cells were removed from 70% EtOH storage at -20 °C. Coverslips were air-dried to remove all traces of EtOH and rehydrated in 2× SSC for 5 minutes. Samples were then hybridized overnight at 1 nM probe concentration in 10% hybridization buffer at 37 °C. 10% hybridization buffer is composed of 10% formamide (Ambion, Cat. # AM9342), 10% Dextran Sulfate (Sigma-Aldrich, Cat. # D6001) and 2× SSC (Sigma-Aldrich, Cat. # 93017) in RNAse-Free H_2O (Life Technologies, Cat. # 10977-015). While higher concentrations of probe often generate more signal per mRNA molecule, the corresponding increase in background generally negates any advantages.

Probe wash

Following hybridization, samples were washed in a solution of 30% formamide, 2× SSC, 0.1% Triton-X 100 (Sigma-Aldrich, Cat. # T8787) for at least 15 minutes. Increasing the wash duration appeared to have little effect on signal or background. All traces of wash buffer and unbound probe were removed by multiple rinses in 2× SSC.

HCR amplification
During the wash step above, fluorophore-labeled HCR hairpins purchased from Molecular Instruments (molecularinstruments.org) were thawed out of -20 °C storage and snap-cooled (heat at 95 °C for 2 minutes and cool to room temperature for 30 minutes) before use. Amplification was performed for 45 minutes at room temperature at a concentration of 120 nM per hairpin in an amplification buffer consisting of 10% Dextran Sulfate and 2 × SSC in RNAse-Free water. Amplification times can be varied to modify polymer length. Following amplification, samples were washed in the wash buffer described above for at least 10 minutes to remove unbound hairpins.

Imaging
After amplification, samples were briefly stained with DAPI (Life Technologies, Cat. # D1306), rinsed in 2× SSC and placed in an enzymatic anti-bleaching buffer described in Lubeck et al., 2014. Samples were imaged on Nikon Ti-Eclipse microscopes. Due to the high gain of smHCR, samples could be easily imaged on microscopes equipped with either a solid state laser or a xenon arc lamp. All publication data was obtained using laser illumination. All microscopes used high quantum efficiency (QE) Andor iKon-M cameras, but in principle, lower QE cameras can be used to image smHCR.

Image Processing and Analysis
All image analysis was performed on three-dimensional image stacks in MATLAB. Before image analysis, the background in each image was subtracted using the ImageJ rolling ball background subtraction algorithm with a radius of 3 pixels. Next, regions of interest were selected to avoid issues of non-uniform illumination and spherical aberrations on the edges on images. The images were then corrected for chromatic aberrations by using multi-spectral beads to determine a geometric transformation to align all channels. Once the images were sufficiently aligned, local maxima within the image were found after first thresholding the images based on previously published smFISH thresholding methods (Raj et al., 2008). Transcripts for smFISH images were found using previously published LOG filter and local maxima finding methods (Raj et al., 2008).

Transcripts for smHCR images were found by setting all pixels values below a threshold to zero and then finding local maxima. A mask of shape [1 1 1; 1 0 1; 1 1 1] is used to dilate (MATLAB function "imdilate") the grayscale image. The center of the mask is positioned at each pixel, and the pixel value is replaced by the maximum value found at the neighboring pixels where there is a value of 1 in the 3-by-3 matrix. The resulting image is such that every pixel value is replaced by the maximum value of its 8 neighbors. The resulting image is compared to the original image such that every pixel that is greater in the original image than in the dilated imaged is a local maxima of the image. Due to the differing profiles of the smHCR dots from the smFISH dots, LOG filtering to find HCR dots often results in errors in dot positions. Once dots were found in all images, the local maxima were matched using a maximum 1-pixel tolerance symmetric nearest neighbor search (SNNS). SNNS only matches dots that are the closest to each other and not to any other point. Analysis software can be obtained upon request.

We define true mRNA signals as those dots that are colocalized in at least two of the three channels. We calculate a true positive rate for channel x as the percentage of true mRNA signals detected as dots in channel x:

$$\%TP_x = 100 N_x^{true} / N_{mRNA}$$

where N_x^{true} is the number of dots representing true mRNAs detected in channel x, and N_{mRNA} is the total number of true mRNAs detected across the three channels. We calculate a false positive rate for channel x as the percentage of dots in channel x that are not true mRNA signals:

$$\%FP_x = 100 N_x^{false} {}_x / (N_x^{true} + N_x^{false})$$

where N_x^{false} is the number of dots detected in channel x that do not represent true mRNAs (i.e., dots in channel x that do not colocalize with dots in either of the other channels).

Whole-mount zebrafish embryos

The following protocol is adapted from Choi et al., 2014.

Sample Preparation

1. Collect zebrafish embryos and grow in a petri dish with egg H_2O at 28 °C until ~27 h post-fertilization (27 hpf).
2. Dechorionate embryos, transfer to an eppendorf tube and remove excess egg H_2O.
3. Fix zebrafish embryos in 1mL freshly prepared 4% paraformaldehyde (PFA) for 24 hr at 4 °C.
4. Wash embryos 3 x 5 min with PBS to stop the fixation. Fixed embryos can be stored at 4 ºC at this point.
5. Dehydrate and permeabilize with a series of methanol (MeOH) washes:
    a. 100% MeOH for 4 x 10 min
    b. 100% MeOH for 50 min.
6. Rehydrate with a series of graded MeOH / PBST washes for 5 min each:
    a. 75% MeOH / 25% PBST
    b. 50% MeOH / 50% PBST
    c. 25% MeOH / 75% PBST
    d. 5 x 100% PBST
7. Store embryos at 4 °C before use.

In situ hybridization

Probe design and synthesis

smHCR probes for the mRNA target (*kdrl*) are 71 nt long (30-nt mRNA recognition sequence, 5-nt spacer, 36-nt initiator). Each probe set contains 39 1-initiator DNA probes (Table S3; sequences listed 5' to 3'). Probes were designed to have ≥ 5 nt gaps between each other along the target mRNA. The order of probe binding is alternating between probe sets along the mRNA. Within a given probe set, each probe initiates the same DNA HCR amplifier. Probes were purchased from Molecular Instruments.

Probe hybridization

1. Pre-hybridize approximately 6 embryos in pre- hybridization buffer for 30 min at 65 °C. Pre-hybridization buffer is composed of 50% formamide (Ambion, Cat. # AM9342), 5× SSC (Invitrogen, Cat. # 15557-044), 9 mM citric acid pH 6 (Mallinckrodt Chemicals, Cat. # 0627-12), 0.1% Tween-20 (Bio-Rad, Cat. # 161-0781), 50 µg/mL heparin (Sigma, Cat. # H3393), 1× Denhardt's solution (Invitrogen, Cat. # 750018) and 10% dextran sulfate (Sigma, Cat. # D6001).

2. Meanwhile, prepare the probe solution:
    a. Each probe should be at a concentration of 2 nM.
    b. Create a probe mixture in probe hybridization buffer of the desired volume. Hybridization buffer composition is identical to the pre-hybridization buffer with 30% formamide instead of 50%.
    c. Warm the mixture to 37 °C.

3. Remove the pre-hybridization solution from samples and add the probe solution.

4. Incubate overnight (>12 hrs) at 37 °C.

Probe wash

Following hybridization, samples were washed at 37 °C in a series of graded probe wash buffer / 5× SSCT. Probe wash buffer is composed of 30% formamide, 5× SSC, 9 mM citric acid pH 6, 0.1% Tween-20, and 50 µg/mL heparin.

1. 75% probe wash buffer / 25% 5× SSCT for 15 minutes
2. 50% probe wash buffer / 50% 5× SSCT for 15 minutes
3. 25% probe wash buffer / 75% 5× SSCT for 15 minutes
4. 100% 5× SSCT for 15 minutes
5. 100% 5× SSCT for 30 minutes

HCR amplification

1. Pre-amplify samples in amplification buffer (5x SSC, 0.1% Tween-20, 10% dextran sulfate) for 30 min at room temperature.

2. Meanwhile, prepare the hairpin solution:

a. Hairpins should first be snap cooled **individually** at the provided concentration – 3 µM. Only snap cool the amount of hairpin required for this experiment: hairpins are used at a final concentration of 60 nM.

b. Snap cool **each hairpin separately** by heating to 95 °C for 90 seconds and cooling to room temperature in a dark drawer for 30 min.

c. Mix the two hairpins together in amplification buffer to achieve a final concentration of 60 nM for each hairpin.

3. Remove the pre-amplification solution from samples and add the hairpin solution.

4. Incubate the samples for 1 hr at room temperature.

Hairpin washing

Remove excess hairpins by washing at room temperature:

1. 2 x 5 min of 5x SSCT

2. 2 x 30 min of 5x SSCT

3. 1 x 5 min of 5x SSCT

Imaging

Prior to imaging, the 5× SSCT was replaced with SlowFade Gold Antifade Mountant with DAPI (ThermoFisher Scientific, Cat. # S36937). The head and yolk sac were resected and fish tails were mounted sandwiched between two no. 1 coverslips (VWR, Cat. # 48393-106). Images were collected on an Andor CSU-W1 spinning disk confocal on a Nikon Ti-E with Perfect Focus System microscope equipped with a Plan Apo λ 60×/1.4 and an Andor iXon ULTRA 888BV camera.

Image Processing and Analysis

Image processing and analysis is performed as described above for cell culture.

Adult mouse brain slices

Animals

Mice (see Sample Preparation) were housed and cared for in accordance with the Guide for the Care and Use of Laboratory Animals (National Research Council (U.S.) in an AAALAC accredited facility. All research protocols were approved by the Institutional Animal Care and Use Committee (Caltech, Pasadena, CA).

Sample Preparation

All procedures were done in an RNase-free environment. Adult mice (8-14 weeks old, C57BL/6N-Tac1-IRES2-Cre-D or C57BL/6J Thy1-yfp) were subjected to standard transcardiac perfusion with ice-cold 4% PFA in 1x PBS followed by brain extraction and post-fixation in 4% PFA for 2-3 hours at room temperature (RT). Using a vibratome (VT1200S, Leica) or a mouse brain matrix (Kent Scientific Corp., Cat. # RBMS-200C), the brain was cut into 0.25-1 mm thick slices, and further post-fixed for an additional 2-4 hours at RT in order to better preserve mRNA transcripts.

PACT clearing

The above PFA-fixed brain slices were then PACT cleared following the previously reported protocol (Yang et al., 2014, Treweek et al., 2015). Briefly, the slices were incubated in hydrogel monomer solution containing either 4% acrylamide (A4P0) or, for better protein and RNA retention, 4% acrylamide with 1% PFA (A4P1) in 1x PBS supplemented with 0.25% photoinitiator 2,2'-Azobis[2-(2-imidazolin-2-yl) propane] dihydrochloride (VA-044) (Wako Chemicals USA, Cat. # 011-19365) at 4 °C overnight. The following day the samples were rigorously degassed using nitrogen gas for 8-10 minutes, and the tissue-gel hybrid was constructed at 37 °C for ~3 hours. After multiple rounds of 1x PBS washes, the samples were transferred to 50 mL conical tubes pre-filled with detergent solution (8% SDS in 1x PBS, pH 7.6), and incubated at 37 °C for 1-3 days until the samples were optically transparent. Before HCR in situ hybridization, the brain slices were extensively washed with 1x PBS for 2-3 days in order to remove residual SDS in the sample.

In situ hybridization

Probe design and synthesis

Probes for the *Pgk1* transcripts hybridized in mouse brain slices are the same probe set as used for cultured CAD cells. For all smHCR probes, each probe contains 20-nt mRNA recognition sequence designed using Stellaris Designer, 4-nt spacer, and 36-nt initiator. The probe set contains 21-32 DNA probes (Table S4).

Probe hybridization

smHCR was performed in a 24 well plate, and during hybridization each well was filled with 2-ml buffer solutions and constantly shaking by a 3D rotating mixer. Each slice of brain samples was transferred to an individual well, and first pre-incubated in 2× SSC for 1 hour followed by the incubation of hybridization buffer (10% formamide, 10% dextran sulfate, 2× SSC) containing DNA HCR probes (1-5 nM per probe) overnight (>12 hrs) at 37 °C.

Probe wash

The following day, the samples were washed by three rounds of wash buffer (30% formamide, 2× SSC at 37 °C for 30 minutes in each round) to remove free and nonspecifically-bound probes. Samples were then rinsed with 2 more rounds of 2× SSC solution at RT.

HCR amplification

The HCR amplification stage was performed according to the next-generation HCR protocol (Choi et al., 2014). At the amplification stage, in a 24-well plate each well was filled with 500 μl of amplification buffer (minimum amount of buffer volume sufficient to cover the entire brain slice) consisting of 10% Dextran Sulfate, 2× SSC, and the amplifier hairpins at a concentration of 120 nM. Amplification in 0.25-1 mm brain slices was performed for 5-6 hours (RT) and incubated on a rotating shaker (~70 rpm). Samples were then washed with 2x SSC for 2-3 times.

Imaging

The sample slices were stained with DAPI for 10 minutes, rinsed with 2x SSC for 2-3 times, and then placed in an enzymatic anti-bleaching buffer consisting of 10 mM Tris-HCl, 0.8% Glucose, and Pyranose oxidase (Sigma P4234) prepared either in 2x SSC for confocal microscopy or in RIMS (final refractive index of 1.47) for SPIM imaging.

Spinning-disk confocal microscopy

Brain slices were mounted and sandwiched between two No. 1 coverslips (EMS, Cat. # 63768-01). Images were collected on an Andor CSU-X spinning disk confocal on an Olympus IX81 microscope equipped with Andor iKon-M camera. The images were acquired by an oil immersion objective (Olympus UPLSAPO 60x, NA 1.35, w.d. 0.15).

SPIM

SPIM images were acquired using a custom built microscope for tissue clearing applications (Tomer et al., 2014, Keller et al., 2010, Treweek et al., 2015). Prior to mounting, the brain slices in RIMS solution containing the anti-bleaching buffer were degassed by nitrogen gas for ~30 minutes. After degassing, the sample and the degassed solution were quickly transferred to in a Spectrosil Quartz cuvette (Fisher scientific, Cat. # NC9520499), and the brain slices were positioned on the cuvette wall by inserting another thin glass slide inside the cuvette. The cuvette was then attached to a translation stage that can lower the sample to the imaging chamber pre-filled with 100% glycerol or RIMS (refractive index of 1.47). The images were acquired by our custom built microscope, and the SPIM design and the optical components can be found in Treweek et al., (2015). Briefly, the channels of YFP, Cy3B, alexa 647 and IR800 fluorophores were excited using 473 nm, 561 nm, 640 nm, and 730 nm lasers, respectively. The emitted light was collected using a 10x CLARITY objective (NA 0.6, Olympus) in Fig. 4A and Movie 1, or a 25x CLARITY objective (NA 1.0, Olympus) in all other SPIM images. The images were digitized using a 4-megapixel cMOS camera (Andor Zyla 4.2), at a frame rate of 25 frames per second. To speed up the processing time, the pixels were binned (2x2) for images in Fig. 4A and Movie 1. When multiple tiles were acquired, TeraStitcher was used to stitch the images (Bria and Lannello, 2012).

Image Processing and Analysis

For SPIM dot analysis, the images were first registered using MATLAB command imregdemons, which calculates a 3D displacement field to maximally align individual channels. Once, the channels are aligned, the background is then subtracted as explained previously. A Laplacian of Gaussian (LoG) filter was then applied to the resulting images. Dots were then identified using MATLAB's local maxima finder (imregionalmax).

Simultaneous Endogenous EYFP and HCR detection in PACT-Cleared Brain Slices

To test the sample depth limit of SPIM, 1-mm thick brain slices from a Thy1-YFP mouse were PACT cleared and hybridized with HCR probes against YFP mRNA (see Fig. S1 for flow diagram).

As PACT cleared tissue retains endogenous YFP fluorescence, we were able to directly test the selectivity of HCR without the need for parallel antibody staining (Figs S13-S16, Movie 3). Fig. S15 illustrates the change of the mean intensity as a function of imaging depth, without the use of intensity normalization. The Thy1-YFP expressing cells (green) account for less than 5% of the cellular population (Fig. S16) and we observe a one-to-one correspondence between cells visualized by endogenous YFP protein fluorescence and cells stained for *YFP* mRNA by smHCR. For this transcript, the expression level is sufficiently high that we do not observe individual dots.
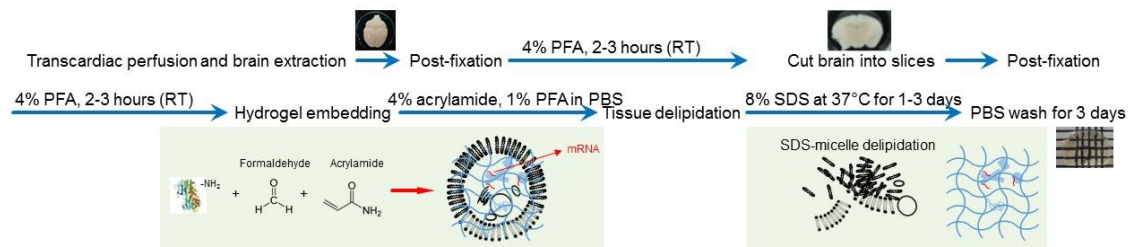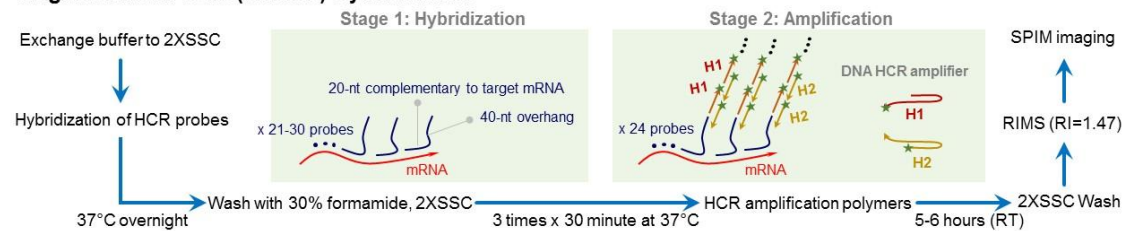
Figure S1. PACT-clearing and smHCR protocol overview. (Top) PACT flow chart. The main refinements from the standard PACT protocol (Yang et al., 2014) is an additional fixation step after brain slicing and a hydrogel formulation of A4P1 (Treweek et al., 2015), both in order to better preserve mRNA transcripts. (Bottom) smHCR flow chart. The PACT-cleared brain slices were first hybridized with DNA HCR probes (probe concentration: 1-5 nM) at 37 °C overnight, and washed in high-stringency conditions (30% formamide, 2× SSC at 37 °C for 1.5 hours) to remove the free and nonspecifically-bound probes. During HCR amplification, hairpins (120 nM) were added to the sample and incubated for 6 hours at RT. The HCR brain slices were then imaged in RIMS (refractive index 1.47; Yang et al., 2014; Treweek et al., 2015) using SPIM microscope (Treweek et al., 2015).
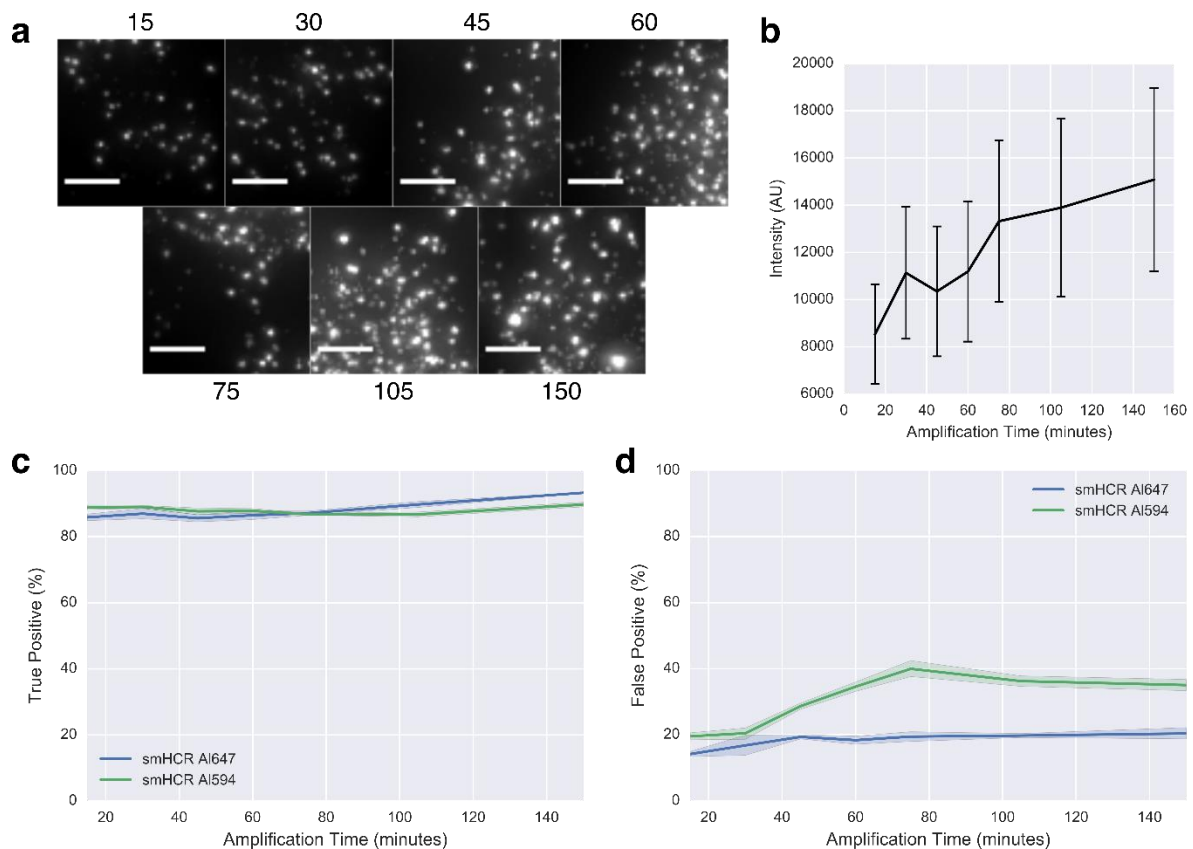
Figure S2. Single molecule HCR behavior as a function of time. **(a)** Images of mRNA transcript signals for Pgk1 transcripts at various amplification times. Images at 15, 30 and 45 minutes show mostly diffraction-limited dots. Images at 60 mins and longer show mostly non-diffraction limited dots. **(b)** Median true positive dot intensity as a function of time. **(c)** True positive rate as function of amplification time. **(d)** False positive rate as function of amplification time. Target mRNA: Pgk1. Sample: cultured CAD cells. N = 5 wells.
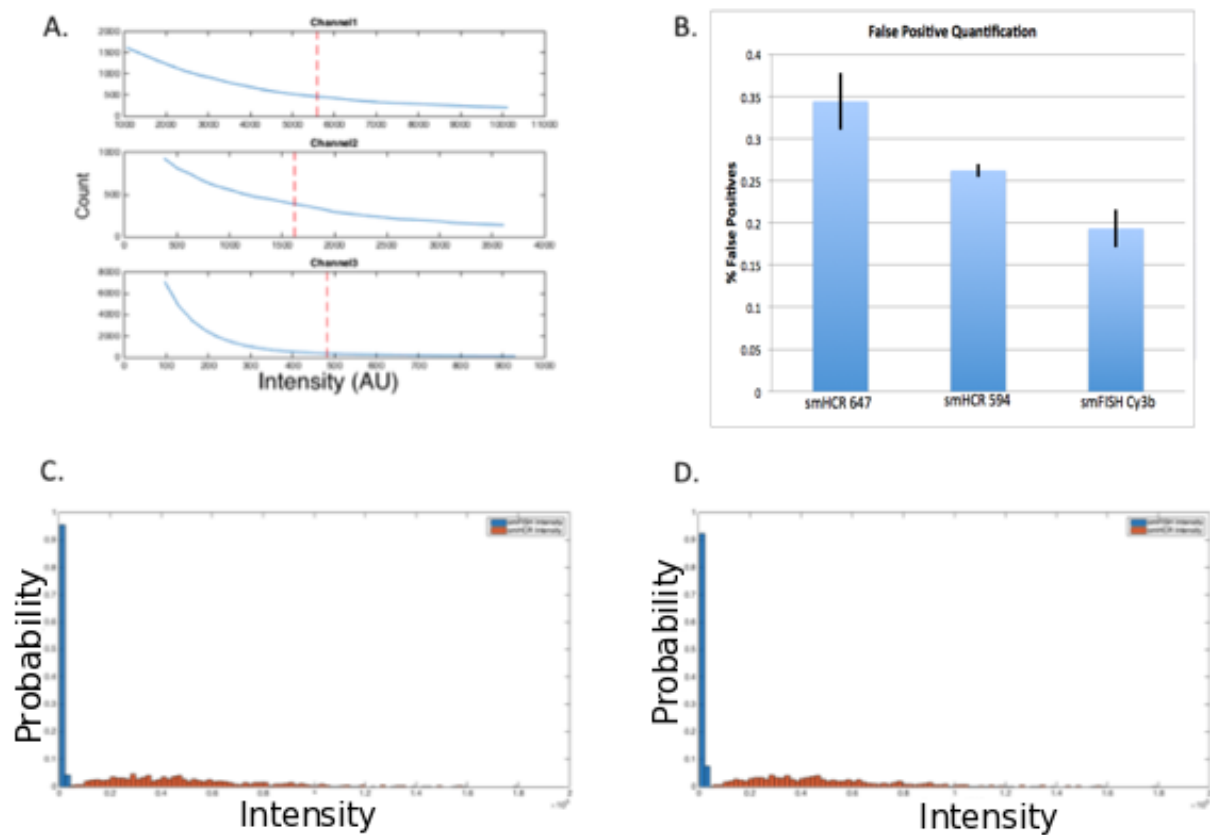
Figure S3. A. Thresholding for the 3-channel colocalization studies of Figure 1cd. Channel1 = smHCR B1 Alexa647, Channel2 = smHCR B3 Alexa594, Channel3 = smFISH Cy3B. Dashed lines depict thresholds selected for Figure 1cd. **B.** Quantification of false positives for the three-channel colocalization studies of Figure 1cd. A dot that is present in only one channel is interpreted as a false positive in that channel. **C.** Comparison of smFISH (Alexa 647) and smHCR (DNA HCR B1-Alexa 647) true-positive dot intensities. The ratio of median signal intensities is 36. Single molecule HCR intensity distribution is shown in orange and smFISH is shown in blue. **D.** Comparison of smFISH (Alexa 594) and smHCR (DNA HCR B3-Alexa 594) true-positive dot intensities. Single molecule HCR intensity distribution is shown in orange and smFISH is shown in blue. The ratio of median signal intensities is 13. Target mRNA: *Pcdh α*. Sample: cultured CAD cells.
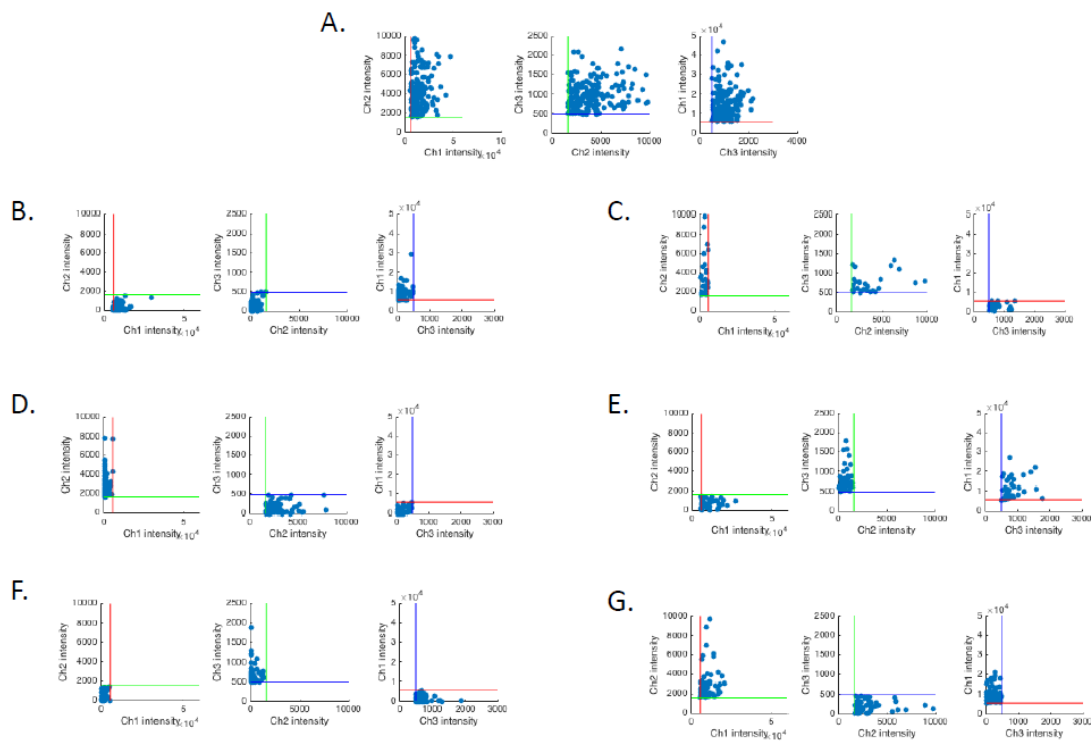
Figure S4. A. Pairwise intensity of true-positive dots colocalized in all three channels in the study of Figure 1cd. **B.** Pairwise intensity of false-negative dots in Channel 1 for colocalization study of Figure 1cd. A dot that is absent in only one channel is interpreted to be a false negative in that channel. **C.** Pairwise intensity of false-positive dots in Channel 1 for colocalization study of Figure 1cd. A dot that is present in only one channel is interpreted to be a false positive in that channel. **D.** Pairwise intensity of false-negative dots in Channel 2 for colocalization study of Figure 1cd. **E.** Pairwise intensity of false-positive dots in Channel 2 for colocalization study of Figure 1cd. **F.** Pairwise intensity of false-negative dots in Channel 3 for colocalization study of Figure 1cd. **G.** Pairwise intensity of false-positive dots in Channel 3 for colocalization study of Figure 1cd. Plots **B**, **D**, and **F** show that all transcripts are mostly detected via smHCR and smFISH, but the false positives are due to the fact that the intensities of these dots are set below the threshold value for true positive detection. The transcripts only detected in 2 out of three channels have a pair in the third channel, but that dot is below the determined noise floor. Also, plots **C, E,** and **G** show that some false positive dots also may be true positives with corresponding intensities in the other two channels being below the noise threshold. Dot intensities depicted as the maximum pixel intensity. Channel thresholds depicted as colored lines: Red line = Ch1 threshold, Green line = Ch2 threshold, Blue line = Ch3 threshold. Ch1 = Alexa 647 smHCR, Ch2 = Alexa 594 smHCR, Ch3 = Cy3B smFISH. Target mRNA: *Pcdh α*. Sample: cultured CAD cells.
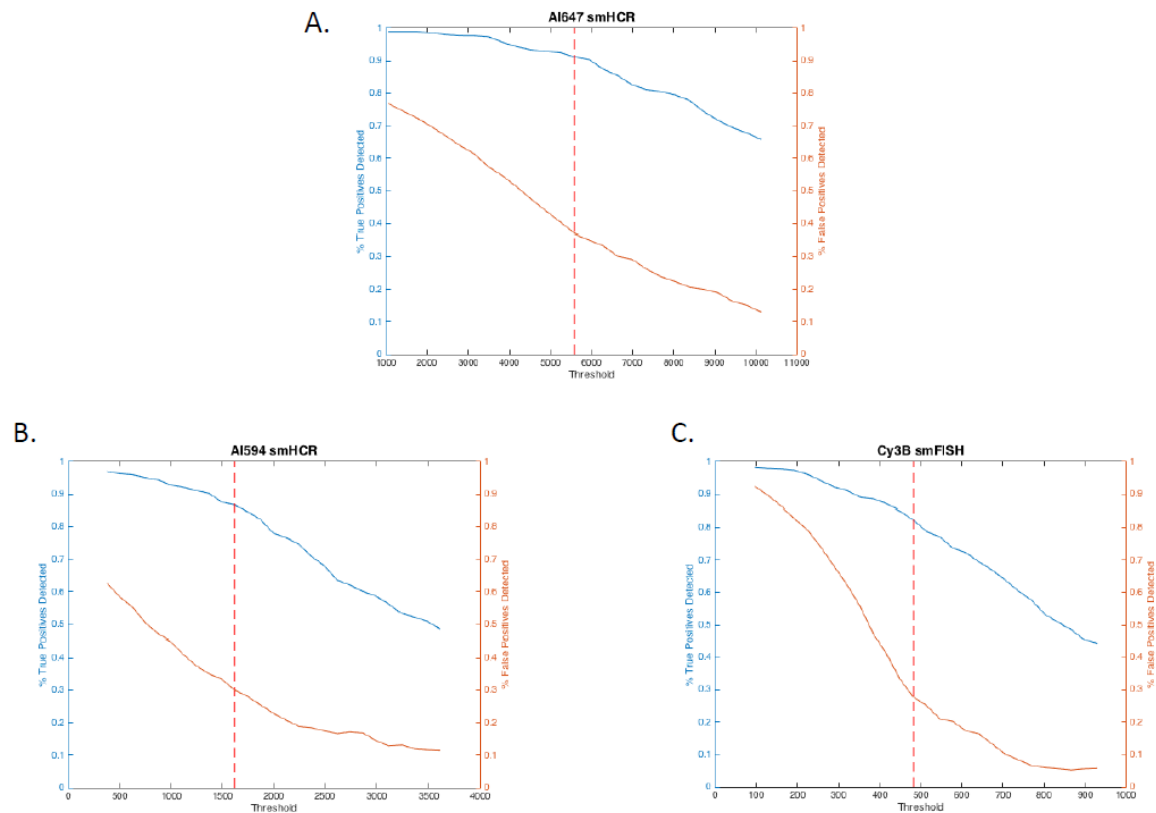
Figure S5. A. Tradeoff between sensitivity and selectivity (Channel 1; Alexa 647 smHCR) as a function of pixel intensity threshold for the three-channel colocalization study of Figure 1cd. **B.** Tradeoff between sensitivity and selectivity (Channel 2; Alexa 594 smHCR) as a function of pixel intensity threshold for the three-channel colocalization study of Figure 1cd. **C.** Tradeoff between sensitivity and selectivity (Channel 3; Cy3B smFISH) as a function of pixel intensity threshold for the three-channel colocalization study of Figure 1cd. Dots that are present in at least two of the three channels are classified as true positives. A dot that is absent in only one channel is interpreted as a false negative in that channel; a dot that is present in only one channel is interpreted as a false positive in that channel. Threshold used for Figure 1cd depicted as a dashed line. Decreasing the threshold increases true positives (improving sensitivity) at the cost of increasing false positives (damaging selectivity). If each target is detected in two channels, false positives can be discarded based on colocalization information, enabling near-quantitative sensitivity. Target mRNA: *Pcdh α*. Sample: cultured CAD cells.
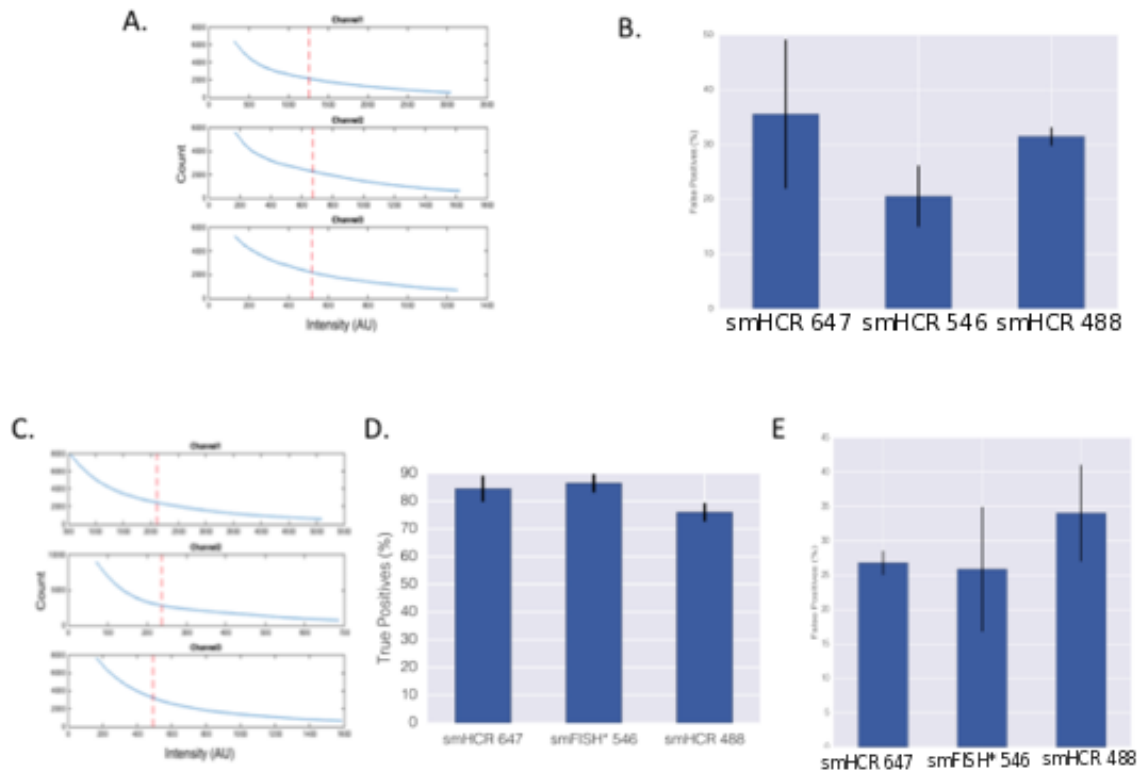
Figure S6. **A.** Thresholding for the 3-channel colocalization studies of Figure 2a. Channel1 = smHCR Alexa647, Channel2 = smHCR Alexa546, Channel3 = smHCR Alexa488. Dashed lines depict thresholds selected for Figure 2a. **B.** Quantification of false positives for the three-channel colocalization studies of Figure 2a. A dot that is present in only one channel is interpreted as a false positive in that channel. **C.** Thresholding for the 3-channel colocalization studies of Figure 2c. Channel1 = smHCR Alexa647, Channel2 = smFISH* Alexa546, Channel3 = smHCR Alexa488. Dashed lines depict thresholds selected for Figure 2c. **D.** Quantification of true positives for the three-channel colocalization studies of Figure 2c. Dots that are present in at least two of the three channels are classified as true positives. A dot that is absent in only one channel is interpreted as a false negative in that channel and as a true positive in the other two channels. **E.** Quantification of false positives for the three-channel colocalization studies of Figure 2c. A dot that is present in only one channel is interpreted as a false positive in that channel. Target mRNA: *kdrl.* Sample: whole-mount zebrafish embryo.
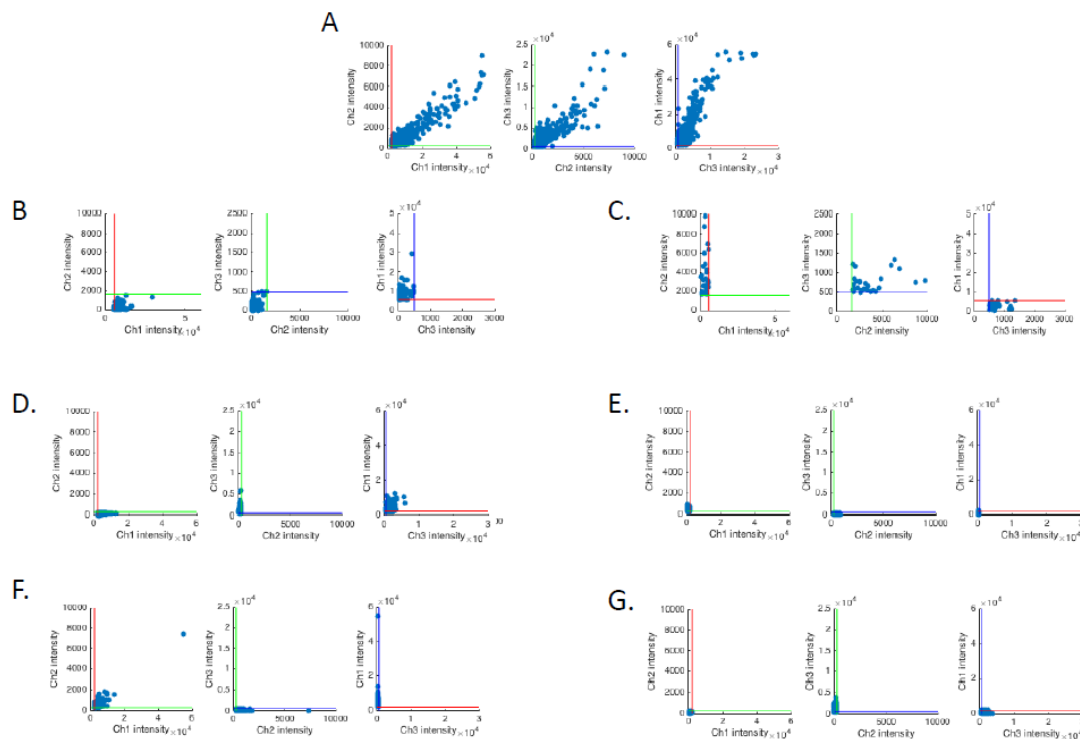
Figure S7. **A.** Pairwise intensity of true-positive dots colocalized in all three channels in the study of Figure 2c. A dot that is present in only one channel is interpreted to be a false positive in that channel. **B.** Pairwise intensity of false-negative dots in Channel 1 for colocalization study of Figure 2c. A dot that is absent in only one channel is interpreted to be a false negative in that channel. **C.** Pairwise intensity of false-positive dots in Channel 1 for colocalization study of Figure 2c. **D.** Pairwise intensity of false-negative dots in Channel 2 for colocalization study of Figure 2c. **E.** Pairwise intensity of false-positive dots in Channel 2 for colocalization study of Figure 2c. **F.** Pairwise intensity of false-negative dots in Channel 3 for colocalization study of Figure 2c. **G.** Pairwise intensity of false-positive dots in Channel 3 for colocalization study of Figure 2c. Plots **B**, **D**, and **F** show that all transcripts are mostly detected via smHCR in all channels, but the false positives are due to the fact that the intensities of these dots are set below the threshold value for true positive detection. The transcripts only detected in 2 out of three channels have a pair in the third channel, but that dot is below the determined noise floor. Also, plots **C**, **E**, and **G** show that some false positive dots also may be true positives with corresponding intensities in the other two channels being below the noise threshold. Dot intensities depicted as the maximum pixel intensity. Channel thresholds depicted as colored lines: Red line = Ch1 threshold, Green line = Ch2 threshold, Blue line = Ch3 threshold. Ch1 = Alexa647 smHCR, Ch2 = Alexa546 smFISH*, Ch3 = Alexa488 smHCR. Target mRNA: *kdrl.* Sample: whole-mount zebrafish embryo.
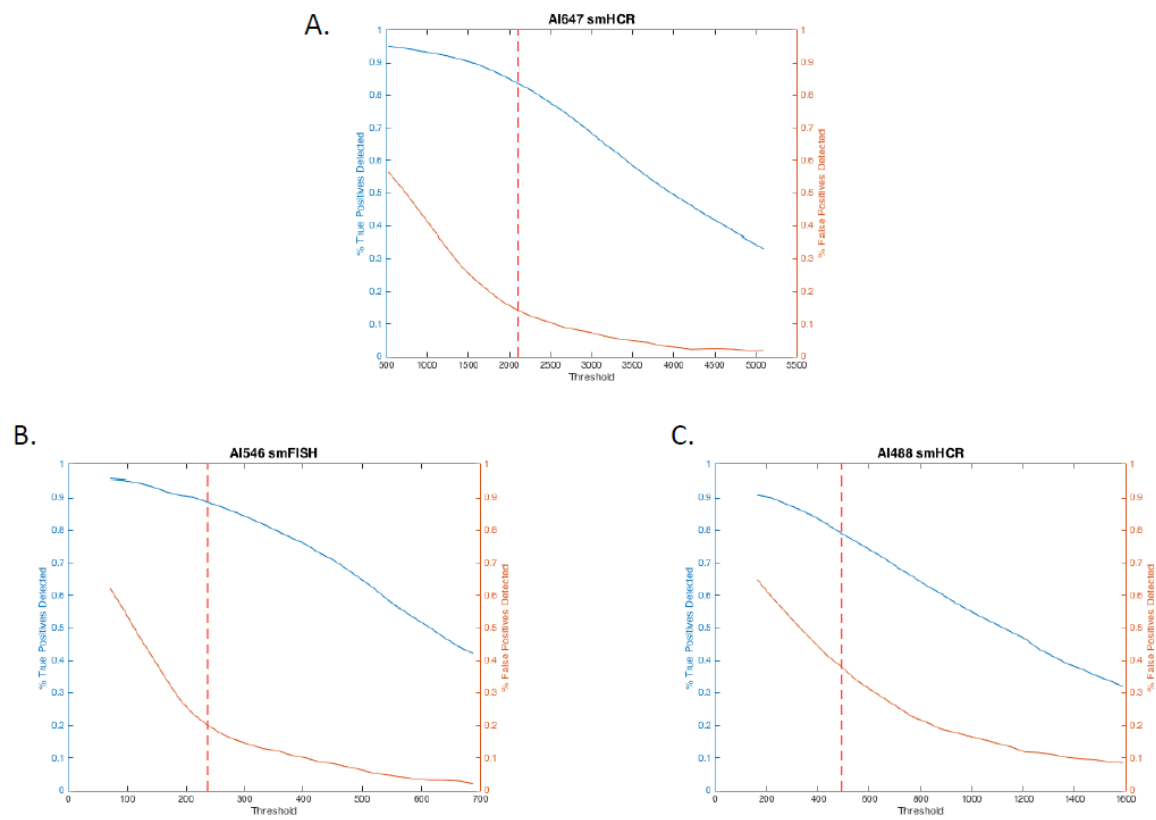
Figure S8. A. Tradeoff between sensitivity and selectivity (Channel 1; Alexa 647 smHCR) as a function of pixel intensity threshold for the three-channel colocalization study of Figure 2c. **B.** Tradeoff between sensitivity and selectivity (Channel 2; Alexa 546 smFISH*) as a function of pixel intensity threshold for the three-channel colocalization study of Figure 2c. **C.** Tradeoff between sensitivity and selectivity (Channel 3; Alexa 488 smHCR) as a function of pixel intensity threshold for the three-channel colocalization study of Figure 2c. Dots that are present in at least two of the three channels are classified as true positives. A dot that is absent in only one channel is interpreted as a false negative in that channel; a dot that is present in only one channel is interpreted as a false positive in that channel. Threshold used for Figure 2c depicted as a dashed line. Decreasing the threshold increases true positives (improving sensitivity) at the cost of increasing false positives (damaging selectivity). If each target is detected in two channels, false positives can be discarded based on colocalization information, enabling near-quantitative sensitivity. Target mRNA: *kdrl.* Sample: whole-mount zebrafish embryo.
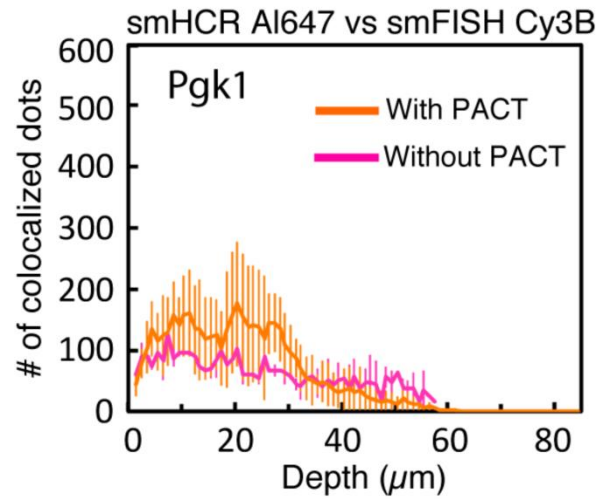
Figure S9. Imaging single mRNAs in adult mouse brain sections using smHCR and PACT. Effect of PACT clearing on the absolute number of colocalized dots for Alexa 647 (smHCR) and Cy3B (smFISH) channels as a function of depth within a 110 μm x 110 μm x 1 μm voxel (median ± median absolute deviation, N = 8 sections with PACT, N = 3 sections without PACT). Target: *Pgk1*. Microscopy: spinning disk confocal. Probe sets: 22 or 23 probes per set, each addressing a 20-nt target subsequence.
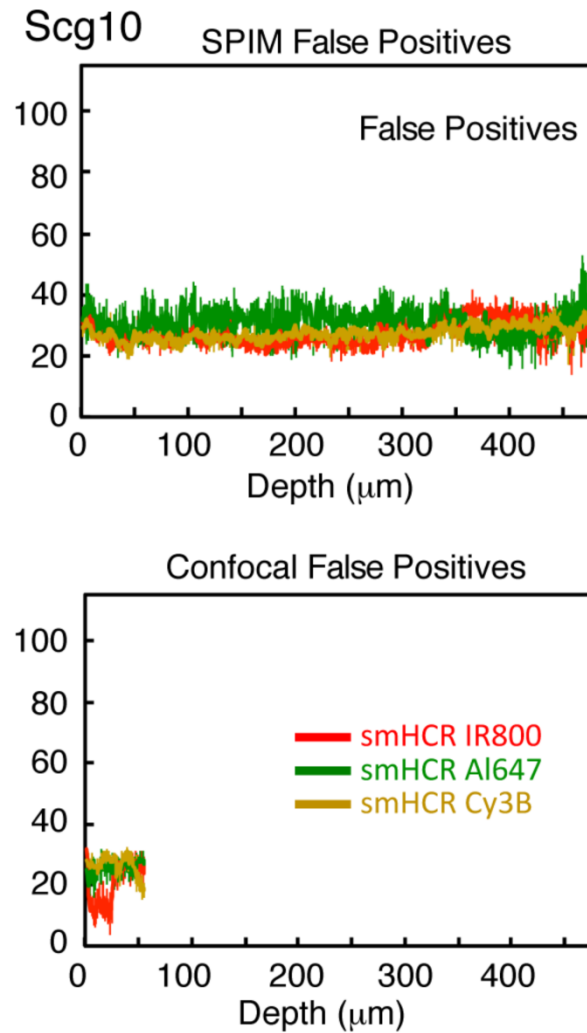
Figure S10. Imaging single mRNAs in thick adult mouse brain sections using smHCR, PACT, and SPIM. False positive rate as a function of depth (median ± median absolute deviation, N = 3 sections from different brains) using SPIM or confocal imaging of *Scg10*. Probe sets: 20 probes per set, each addressing a 20-nt target subsequence.
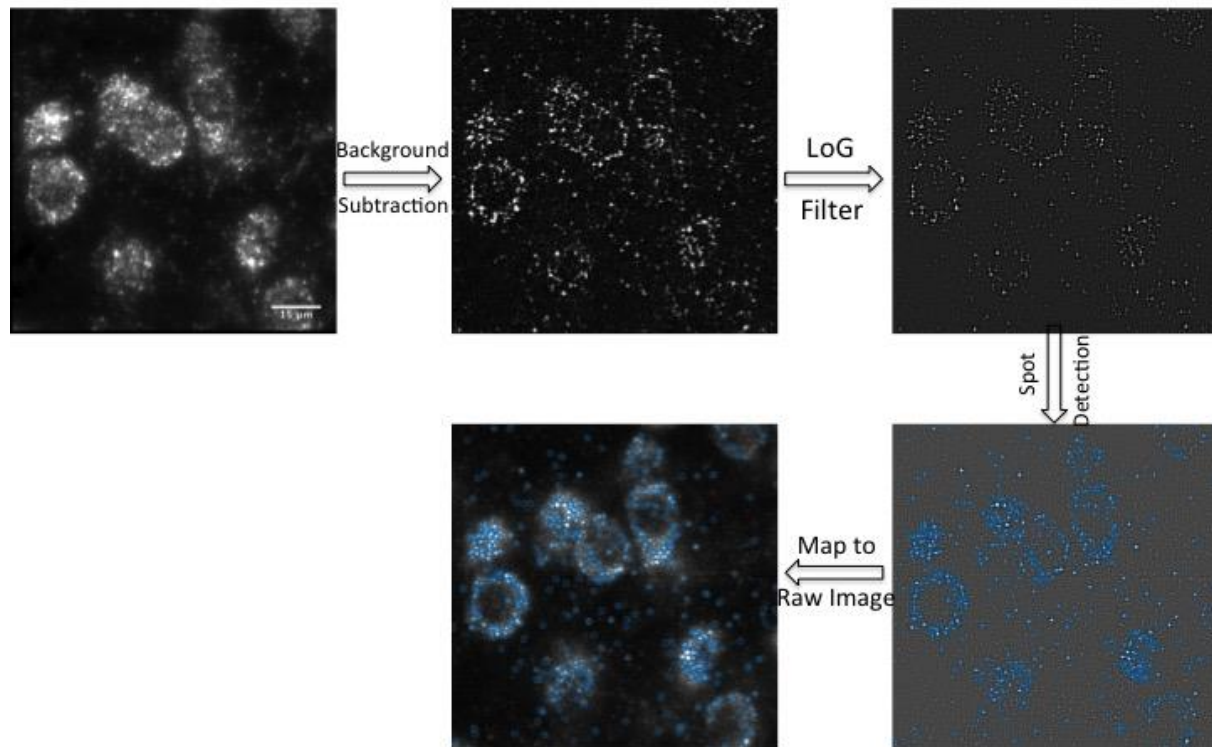
Figure S11. Processing workflow for dot finding in smHCR/PACT/SPIM images. A rolling ball background subtraction algorithm is first used to remove background noise. Next, a Laplacian of Gaussian filter is used to amplify diffraction limited dot signal. Local maxima are found in the resulting image. The locations of the local maxima are mapped back onto the raw image. Processing of the SPIM images in this way finds putative mRNA signals that would otherwise not be obvious to the eye.
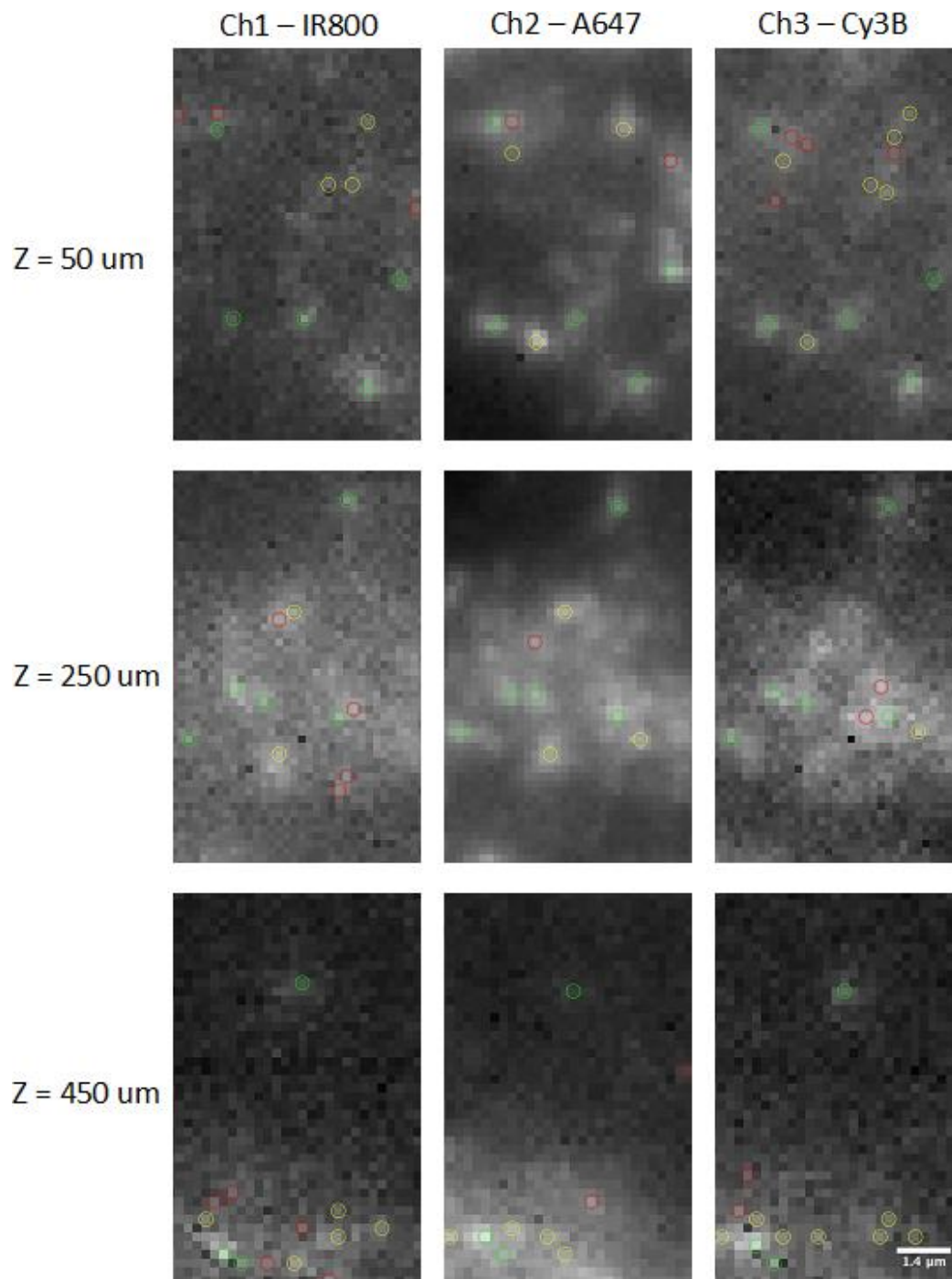
Figure S12. Illustration of dot classification for smHCR/PACT/SPIM data. Dots are classified as triple-detected true positives (present in all 3 channels; green circles), double-detected true positives (present in 2 out of 3 channels; yellow circles), or false positives (present in only one channel; red circles). Circles are superimposed on raw images.
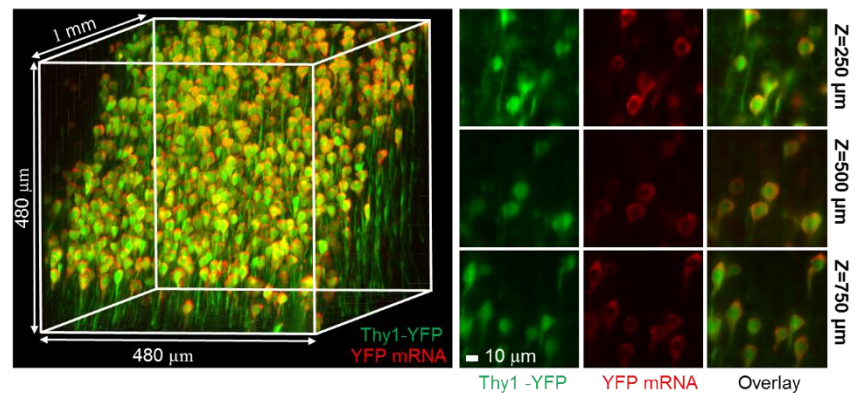
Figure S13. Mapping mRNAs in 1-mm PACT-cleared mouse brain sections using smHCR and SPIM. **(Left)** Three-dimensional reconstruction depicting colocalization of Thy1-YFP protein (expressed in ~5% of cells) and *Thy1-YFP* mRNA (smHCR: Cy3B). **(Right)** Representative optical sections demonstrating that smHCR signal is detected throughout the brain slice (z = 250 μm, 500 μm, 750 μm).
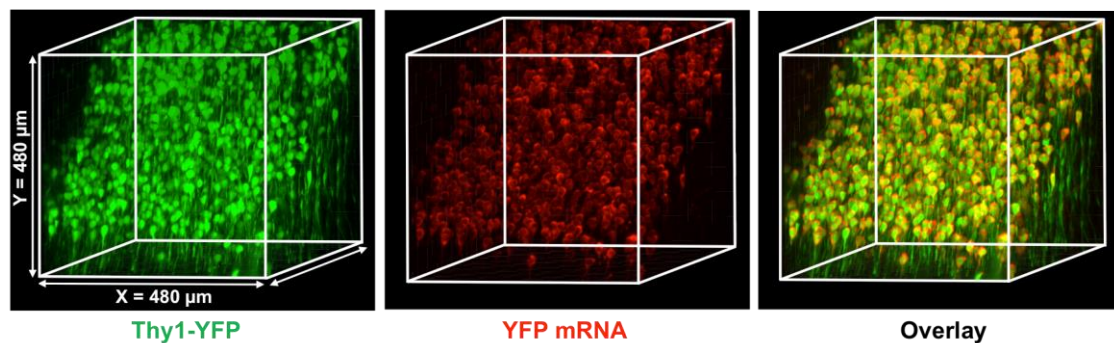

Figure S14. 3D reconstruction of 1-mm PACT-cleared Thy1-YFP mouse brain slice. (Left) Endogenous YFP Protein. (Middle) Cy3B labeling of *YFP* mRNA. (Right) Overlay shows the specificity of the HCR for *YFP* transcripts throughout the thick 1-mm slice.
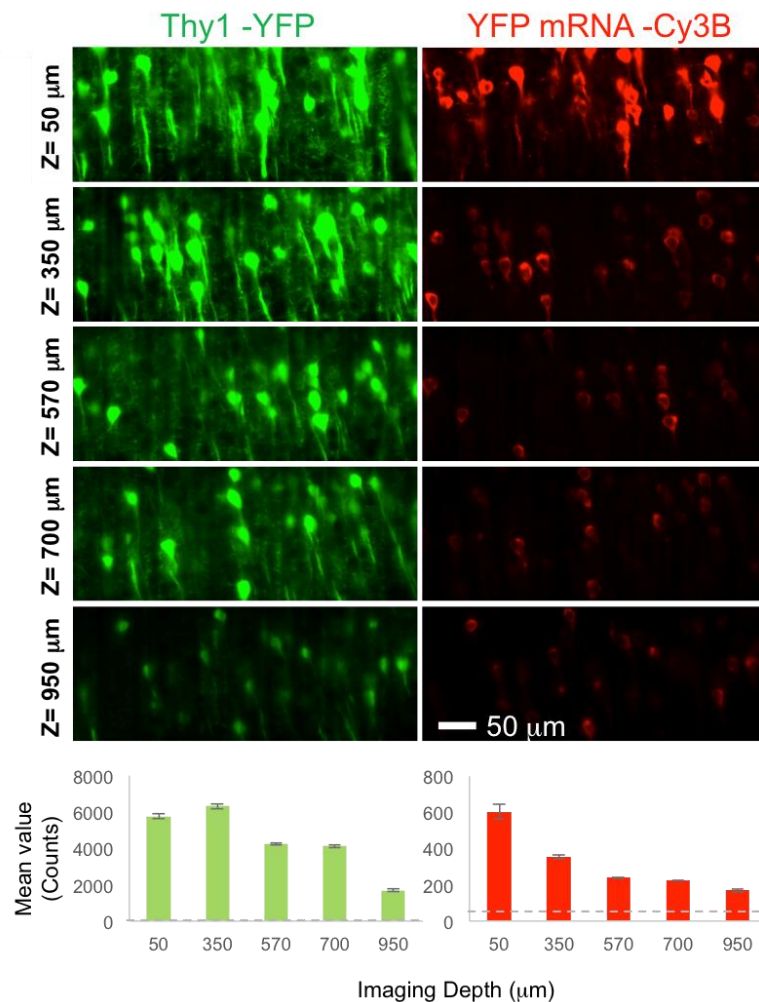
Figure S15. Fluorescence intensity decreases as a function of tissue depth. Attenuation in the fluorescence signal of the YFP and smHCR-Cy3B channels was observed as a function of tissue depth. However, even at 1-mm depth, and without light power compensation, the HCR hybridization still shows a detectable signal that co-localizes with the YFP signal. The dashed line in the lower graph indicates the camera dark count.
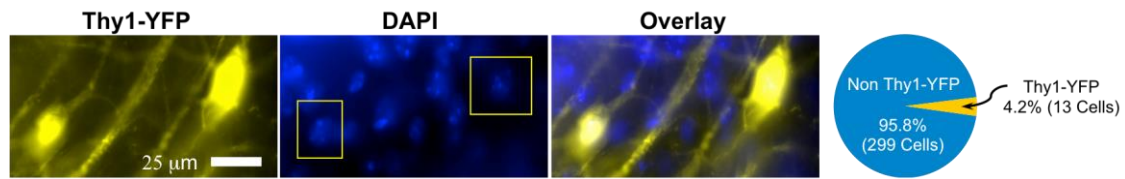
Figure S16. Across a 1-mm cleared Thy1-YFP mouse brain slice, only a small subset of brain cells show YFP expression. (Left) Widefield microscope image (YFP, DAPI, and overlay); yellow boxes in the DAPI image indicate the location of YFP expressing cells. (Right) YFP expressing cells account for less than 5% (13 cells) of the total number of cells (312 cells). Methods: 11 field-of-views of cortical areas (Olympus UPLSAPO 60x, NA 1.35, w.d. 0.15) were processed from a 1-mm Thy1-YFP brain slice. First, a group of YFP expressing cells was located and an image stack (∼50 images with 1 µm spacing) was captured (DAPI and YFP). The volume of each stack was 74 µm × 74 µm × ∼50 µm. Then the number of DAPI stained cells and YFP expressing cells was counted manually.

Table S1.

Click here to Download Table S1

Table S2.

Click here to Download Table S2

Table S3.

Click here to Download Table S3

Table S4.

Click here to Download Table S4

Movie 1: ctgf-mousebrain.mov

3D visualization of Ctgf mRNA in 0.25 mm thick PACT-cleared brain slice. The samples were hybridized with HCR probes against *Ctgf* mRNA and amplified with HCR amplifier B1-IR800. To generate a 3D reconstruction, ~200 optical sections with 1 μm spacing were taken (25 frames per second), and the intensity was normalized between the different sections. Available to download at http://dx.doi.org/10.5061/dryad.31r0d.

Movie 2: scg10-mousebrain.mov

3D visualization of Scg10 mRNA in 0.5 mm thick PACT-cleared brain slice. Related to Figure 3C, representing the colocalization of three smHCR channels (blue, green, and red are the channels of Cy3B, Al647, and IR800 respectively) for target *Scg10*. The movie pauses at z = 33 μm and at z = 445 μm with circles representing true mRNA signals colocalized in two or more of the three channels. About 500 optical sections spaced with 1 μm were taken (10 frames per second), and the intensity was normalized between the different sections. In each channel, the maximum intensity projection of every 5 sections (~5 μm) was used to construct the movie. Available to download at http://dx.doi.org/10.5061/dryad.31r0d.
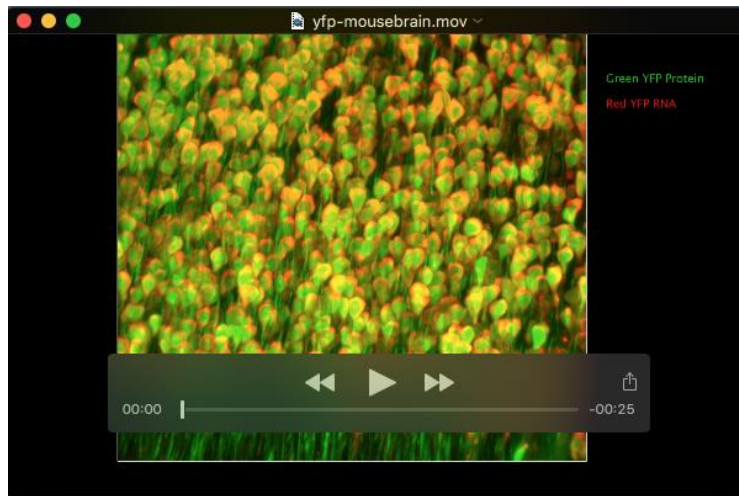
Movie 3: yfp-mousebrain.mov

Simultaneous endogenous EYFP and HCR 3D detection in 1 mm thick PACT-cleared brain slice. Related to Supplementary Figures 13-15. To generate a 3D reconstruction, ~1,000 optical sections with 1 µm spacing were taken (25 frames per second), and the intensity was normalized between the different sections. Available to download at http://dx.doi.org/10.5061/dryad.31r0d.

References

Bria, A. & Lannello, G. (2012). TeraStitcher - A tool for fast automatic 3D-stitching of teravoxel-sized microscopy images. *BMC Bioinformatics* 13, 316.

Choi, H.M.T., Beck, V.A. and Pierce, N.A. (2014). Next-generation in situ hybridization chain reaction: higher gain, lower cost, greater durability. *ACS Nano* 8(5), 4284-4294.

Keller, P.J., Schmidt, A.D., Santella, A., Khairy, K., Bao, Z., Wittbrodt, J., and Stelzer, E.H. (2010). Fast, high-contrast imaging of animal development with scanned light sheet-based structured-illumination microscopy. *Nature Methods* 7, 637-642.

Lubeck, E. & Cai, L. (2012). Single-cell systems biology by super-resolution imaging and combinatorial labeling. *Nature Methods* 9, 743–748.

Lubeck, E., Coskun, A. F., Zhiyentayev, T., Ahmad, M. & Cai, L. (2014). Single-cell in situ RNA profiling by sequential hybridization. *Nature Methods* 11, 360–361.

Raj A, van den Boogard P, Rifkin SA, van Oudenaarden A, Tyagi S. (2008). Imaging individual mRNA molecules using multiple singly labeled probes. *Nature Methods* 5, 877-879.

Suri C, Fung BP, Tischler AS, Chikaraishi DM. (1993). Catecholaminergic cell lines from the brain and adrenal glands of tyrosine hydroxylase-SV40 T antigen transgenic mice. *J Neurosci*. 13(3), 1280-91.

Tomer, R., Ye, L., Hsueh B., and Deisseroth K. (2014). Advanced CLARITY for rapid and high-resolution imaging of intact tissues. *Nature Protocols* 9, 1682-1697.

Treweek, J.B., Chan, K.Y., Flytzanis, N.C., Yang, B., Deverman, B.E., Greenbaum, A., Lignell, A., Xiao, C., Cai, L., Ladinsky, M.S., Bjorkman, P.J., Fowlkes, C.C. and Gradinaru, V. (2015). Whole-Body Tissue Stabilization and Selective Extractions via Tissue-Hydrogel Hybrids for High Resolution Intact Circuit Mapping and Phenotyping. *Nature Protocol*s 10, 1860-1896.

Yang, B., Treweek, J.B., Kulkarni, R.P., Deverman, B.E., Chen, C.-K., Lubeck, E., Shah, S., Cai, L., and Gradinaru, V. (2014). Single-Cell Phenotyping within Transparent Intact Tissue through Whole-Body Clearing. *Cell* 158, 1-14.